Interpolation Scheme for Band Structure of Noble and Transition Metals: Ferromagnetism and Neutron Diffraction in Ni†

L. HODGES,* H. EHRENREICH, AND N. D. LANG
Division of Engineering and Applied Physics, Harvard University, Cambridge, Massachusetts
(Received 17 June 1966)

A simple interpolation scheme for paramagnetic fcc transition and noble metals has been developed and extended to the ferromagnetic state of Ni. It is based on the representation of *d* and conduction bands by linear combinations of atomic orbitals and orthogonalized plane waves, respectively, and includes hybridization effects through the use of **k**-dependent matrix elements. The energy bands of augmented-plane-wave calculations from first principles for Cu and paramagnetic Ni are fitted with an rms deviation of about 0.12 eV. The density of states of paramagnetic Ni is calculated and shown to be significantly influenced by hybridization. A self-consistent calculation of the ferromagnetic band structure of Ni is carried out by the incorporation of correlation effects through the use of an intra-atomic Coulomb interaction patterned along the lines suggested by Gutzwiller, Hubbard, and Kanamori. Experimental information relating to the magnetization, ferromagnetic Kerr effect, Fermi surfaces, neutron magnetic form factor, electronic specific heat, and high-field susceptibility is used to determine the parameters characteristic of the ferromagnetic state and to check the predictions of the resulting band structure. The **k**-dependent splitting of the bands averages 0.37 eV in the vicinity of the Fermi level. The wave functions resulting from these calculations are shown to be sufficiently realistic to permit the calculation of the total charge density in Cu and the magnetic form factor of Ni. The use of approximate spin-polarized wave functions appropriate to the solid demonstrates the importance of both unpaired and paired electrons to the magnetic form factor. The net conduction-electron polarization is found to be small and positive. The effective *s-d* exchange energy changes sign between the central and outer parts of the Brillouin zone. The inclusion of spin-orbit effects is discussed, and the reduction of the density of states at the Fermi level due to this interaction is calculated. The effect is too small to explain the presence of ferromagnetism in Ni and its absence in Pd and Pt.

I. INTRODUCTION

THE description of the electronic energy levels of ferromagnetic transition metals in realistic band-theoretic terms represents a fairly recent development[1] for essentially three reasons. First, it was not clear to what extent a view which regards all the *d* electrons in transition metals as itinerant was valid.[2] Second, sophisticated band calculations from first principles for these metals in their paramagnetic state have only become available during the past few years.[3–8] Third, it was not evident how to formulate a tractable, although realistic, form of the Coulomb interaction, which is necessary for describing the electron correlations involved in the ferromagnetic state, nor how the resulting formidable self-consistency problems involved in the solution could be dealt with practically.

Some of these issues have now been resolved. At least for Ni, the existing experimental evidence[1,9] now overwhelmingly favors an itinerant description. The results of band calculations for the noble and the transition metals are now believed reliable. Particularly in the case of Cu, there is available a wide variety of Fermi-surface experiments[10] which agree very well with band calculations. In addition, there is the reassuring fact that the band calculations of Segall[3] and Burdick,[4] based respectively on the Kohn-Rostoker and augmented-plane-wave (APW) methods, yielded substantially the same results. However, it is in regard to the third problem that the progress to date has been most limited. The recognition that correlations among the *d* electrons can be described semiquantitatively in terms of purely intra-atomic Coulomb interactions, because of the screening resulting from the presence of conduction electrons, has been most important.[1,11–15] However, even

† Supported in part by the National Science Foundation under grant GP-5321 and the Advanced Research Projects Agency.
* Present address: Physics Department, Iowa State University, Ames, Iowa.
[1] To avoid the fairly formidable bibliography that would be required in order to summarize the principal contributions responsible for the development of this viewpoint, we cite instead C. Herring, in *Magnetism*, edited by G. Rado and H. Suhl (Academic Press Inc., New York, 1966), Vol. 4, which contains a most comprehensive discussion of these matters, together with a complete set of references. We wish to thank Dr. Herring for sending us the manuscript of this important book prior to publication.
[2] C. Herring, J. Appl. Phys. **31**, 3S (1960); H. Brooks, in *Electronic Structure and Alloy Chemistry of the Transition Elements*, edited by Paul A. Beck (Interscience Publishers, Inc., New York, 1963); N. F. Mott, Advan. Phys. **13**, 325 (1964).
[3] B. Segall, Phys. Rev. **125**, 109 (1962).
[4] G. A. Burdick, Phys. Rev. **129**, 138 (1963).
[5] J. G. Hanus, M.I.T. Solid State and Molecular Theory Group Quarterly Progress Report No. 44, 29, 1962 (unpublished).
[6] L. F. Mattheiss, Phys. Rev. **134**, A970 (1964).
[7] J. H. Wood, Phys. Rev. **117**, 714 (1960); **126**, 517 (1962).
[8] J. Yamashita, M. Fukuchi, and S. Wakoh, J. Phys. Soc. Japan **18**, 999 (1963); S. Wakoh and J. Yamashita, *ibid.* **19**, 1342 (1964).
[9] For example, E. Fawcett and W. A. Reed, Phys. Rev. Letters **9**, 336 (1962); Phys. Rev. **131**, 2463 (1963); E. Fawcett, Advan. Phys. **13**, 139 (1964); A. S. Joseph and A. C. Thorsen, Phys. Rev. Letters **11**, 554 (1963).
[10] For an excellent summary, see *The Fermi Surface*, edited by W. A. Harrison and M. B. Webb (John Wiley & Sons, Inc., New York, 1960). Also, J. F. Koch, R. A. Stradling, and A. F. Kip, Phys. Rev. **133**, A240 (1964).
[11] J. C. Slater, Phys. Rev. **49**, 537, 931 (1936).
[12] J. H. Van Vleck, Rev. Mod. Phys. **25**, 220 (1953).
[13] M. C. Gutzwiller, Phys. Rev. Letters **10**, 159 (1963); Phys. Rev. **134**, A923 (1964).
[14] J. Hubbard, Proc. Roy. Soc. (London) **A276**, 238 (1963); **A277**, 237 (1964); **A281**, 401 (1964).
[15] J. Kanamori, Progr. Theoret. Phys. (Kyoto) **30**, 275 (1963).

after this simplification, one is still left with the problem of dealing adequately with the remaining correlations, and in particular with the degeneracy of the d electrons whose importance to the existence of the ferromagnetic state has been stressed by Van Vleck[16,12] and Herring.[1] At the time of writing, the self-consistency problem alluded to above is beginning to be attacked[17] by band calculations from first principles, but it seems clear that it will be some time until the results of such calculations achieve the same degree of reliability as corresponding paramagnetic calculations.

As an interim measure, one might ask whether pseudopotential (or interpolation) techniques, which have been so successful in elucidating the band structures of semiconductors[18] and simple metals[19] in terms of rather elementary calculations, might not be usefully extended to apply first to the noble and transition metals in their paramagnetic state, and second to ferromagnetic metals by suitably generalizing the band Hamiltonian to include correlation effects. The results of such calculations are valuable, because in permitting a description of the electron energy levels in terms of relatively few adjustable parameters, they facilitate the incorporation of and comparison with a wide variety of experimental information. An optimized choice of such parameters that provides excellent agreement with many experiments and essential contradiction with none would yield an energy level scheme whose over-all validity one would be inclined to trust. Unfortunately, in the case of the transition metals the sort of detailed Fermi-surface results that are now available for the noble metals are still largely lacking, and thus it is impossible to describe with any finality certain details of the energy levels in the immediate vicinity of the Fermi surface. However, any further experimental results are easily incorporated into band calculations utilizing interpolation schemes by means of fine adjustments of the parameters. Another advantage of the application of pseudopotential schemes to ferromagnetic materials is the possibility of testing quantitatively the validity of truncated Coulomb Hamiltonians such as those discussed by Gutzwiller,[13] Hubbard,[14] and Kanamori.[15]

The present paper is devoted to the development of an interpolation scheme applicable to paramagnetic fcc transition and noble metals (particularly Cu and Ni) and its extension to the ferromagnetic state of Ni. The characteristic parameters are adjusted and checked by detailed calculations or discussion of such experimental information as the magneton number,[20] the ferromagnetic splitting of the bands,[1] Fermi surface experiments,[9] magneto-optical experiments,[21] the electronic specific heat,[22] the magnetic form factor as determined from neutron diffraction,[23] and the high-field susceptibility.[24,25] In the exposition of this scheme, we shall also have occasion to incorporate the spin-orbit interaction and to discuss its influence on the density of states at the Fermi surface and hence on the existence of the ferromagnetic state in Ni-related materials such as Pd and Pt.

Since our first report on this subject,[26] Mueller[27] has independently formulated a different sort of interpolation scheme, which is somewhat more accurate than the present one although rather more complicated in its requirement of explicit orthogonalization of conduction-band functions to d functions. It should be emphasized, however, that both techniques yield results which are well within the calculated error associated with first-principles calculations. For example, in Cu, the present method can fit first-principles calculations with an rms deviation of 0.11 eV and maximum error of 0.37 eV, as compared to Mueller's rms value of 0.08 eV. Mueller's work is important in that it delineates the influence of the s-d orthogonalization[28] on the band splittings in the conduction-band portion of the band structure. Heine[29] has recently examined in considerable detail the formal status of such interpolation schemes.

The modifications to be expected in the Ni band structure in passing from the paramagnetic to the ferromagnetic state have been previously discussed in some detail by Ehrenreich, Philipp, and Olechna,[30] and by

[16] J. H. Van Vleck, Nuovo Cimento Suppl. **6**, 857 (1957).

[17] A. C. Switendick, J. Appl. Phys. **37**, 1022 (1966).

[18] J. C. Phillips and L. Kleinman, Phys. Rev. **116**, 287 (1959). From the many papers since written on the subject, we cite only one of the most recent: M. L. Cohen and T. K. Bergstresser, Phys. Rev. **141**, 789 (1966).

[19] For example, W. A. Harrison, *Pseudopotentials in the Theory of Metals* (W. A. Benjamin, Inc., New York, 1966).

[20] C. Kittel, *Introduction to Solid State Physics* (John Wiley & Sons, Inc., New York, 1956), 2nd ed., Chap. 15.

[21] G. S. Krinchik and R. D. Nuralieva, Zh. Eksperim. i Teor. Fiz. **36**, 1022 (1959) [English transl.: Soviet Phys.—JETP **9**, 724 (1959)]; G. S. Krinchik and G. M. Nurmukhavmedov, Zh. Eksperim. i Teor. Fiz. **48**, 34 (1965) [English transl.: Soviet Phys.—JETP **21**, 22 (1965)]; G. S. Krinchik, in *Proceedings of the International Conference on Magnetism, Nottingham, England, 1964* (Institute of Physics and the Physical Society, London, 1965), p. 114.

[22] J. A. Rayne and W. R. G. Kemp, Phil. Mag. **1**, 918 (1956).

[23] H. A. Mook and C. G. Shull, J. Appl. Phys. **37**, 1034 (1966); H. A. Mook, Ph.D. thesis, Harvard, 1965 (unpublished). See Division of Engineering and Applied Physics, Harvard University, Technical Report No. ARPA-17 (unpublished).

[24] A. J. Freeman, N. A. Blum, S. Foner, R. B. Frankel, and E. J. McNiff, Jr., J. Appl. Phys. **37**, 1338 (1966).

[25] C. Herring, R. M. Bozorth, A. E. Clark, and T. R. McGuire, J. Appl. Phys. **37**, 1340 (1966).

[26] L. Hodges and H. Ehrenreich, Phys. Letters **16**, 203 (1965). The conclusions in this letter differ in some respects from those of the present paper, for example in the presence of holes in the majority d band in the earlier publication and their absence here, due to the fact that the parameters characterizing the interpolation scheme had not been adjusted optimally.

[27] F. Mueller, Phys. Rev. **148**, 636 (1966). We are grateful to Dr. Mueller and Professor J. C. Phillips for an unpublished report of this paper.

[28] We shall often refer to the conduction electrons as "s electrons," in reference to the atomic states from which they derive in the noble metals, even though in the solid these electrons contain admixtures corresponding to higher angular momenta.

[29] V. Heine, Phys. Rev. **151**, 561 (1966). We are grateful to Professor Heine for an unpublished report of this paper.

[30] H. Ehrenreich, H. R. Philipp, and D. J. Olechna, Phys. Rev. **131**, 2469 (1963).

Phillips and Mattheis.[31,32] However, the conclusions of this work were based on estimates and speculations, and accordingly have limited reliability. These matters will be discussed and comparison will be made with the results of the present calculations in the appropriate places in this paper. Such a comparison is of interest since the present work, while still containing important approximations and oversimplifications, represents the first time that a reasonably realistic model for Ni, containing most features of the paramagnetic band structure, is calculated out in all detail for the metal in its ferromagnetic state.

Since the present paper is fairly lengthy, it may be useful to summarize the contents of the various sections. Section II presents a general discussion of the interpolation scheme and the various pieces of the underlying Hamiltonian necessary to describe band, ferromagnetic, and spin-orbit properties. The present scheme may be characterized roughly as one that treats the conduction bands in a free-electron-like approximation as suggested by Harrison[33] for Al, the d bands in the tight-binding approximation as in Fletcher's[34] treatment, but with the overlap integrals given by adjustable parameters,[35] and the hybridization integrals as $\mathbf{k}$-dependent functions involving further parameters. Section IIA describes the interpolation scheme in its simplest form, as well as its application to Cu and paramagnetic Ni. Section IIB discusses the inclusion of spin-orbit effects which have previously been discussed only in the absence of hybridization between conduction and d bands.[36] Section IIC discusses a simple but probably fairly realistic model Hamiltonian,[1,13–15] together with some modifications, and its application to the present work.

Section III is devoted to the question of the validity of the wave functions obtained by such interpolation schemes. Ni occupies a somewhat unique position in this respect since the magnetic properties are determined by states near the top of the d bands, where atomic functions serve as an adequate basis for tight-binding wave functions.[7,37] However, such interpolation schemes even provide reasonable (although perhaps not quantitatively valid) results deeper in the d bands. This is illustrated by a calculation of the charge density in Cu and by comparison with results obtained from x-ray experiments,[38] as well as theoretical results of Arlinghaus.[39]

Section IV discusses some implications of the pseudopotential band structures for paramagnetic materials. In particular, we consider the influence of s-d hybridization and of spin-orbit effects on the density of states throughout the entire s-d complex. As a result, it is possible to examine the influence of spin-orbit coupling on the density of states at the Fermi surface for the Ni, Pd, Pt sequence and the question of why only Ni is ferromagnetic.[40] While we do not explicitly discuss the cohesive energy in this paper, it should be noted that this section is pertinent to the role of s-d hybridization in the binding of the solid. This effect has been suggested by Mott[2] to be of possible importance.

Section V deals with the band structure of ferromagnetic Ni and the parameters such as the magneton number, band splittings, and spin-polarization effects characterizing this state. In this connection, it is necessary to discuss some experimental results which are necessary to fit the two extra pseudopotential coefficients that differentiate between the paramagnetic and ferromagnetic band structures. These parameters, the effective d-d polarity and s-d exchange energies, appear in the model Coulomb Hamiltonian that must be appended to the band Hamiltonian in considerations of the ferromagnetic state. This section also deals with the density of states and its implications for a recent controversy concerning high-field susceptibility results.[24,25]

Finally, Sec. VI presents a purely band-theoretic description of the magnetic form factor of Ni,[41] and compares the results with the recent experiments of Mook and Shull.[23] The spin density depends crucially on the wave functions, which ordinarily might not be expected to be as reliable as energy eigenvalues. However, since this density is determined largely by the unpaired electrons near the top of the d bands, one might, in this instance, expect reasonably accurate results if reliable atomic wave functions, such as the unrestricted atomic Hartree-Fock functions of Watson and Freeman,[42] are used as the basis for the Slater-Koster[35] interpolation scheme. Since the conduction-band functions and the wave functions in other regions of the d bands also turn out to be reliable in a semiquantitative sense, it is possible to estimate the conduction-band polarization and the contribution to the spin density of the paired electrons in the remainder of the d band, whose existence depends on the fact that the wave functions corresponding to the two spin directions differ.[43] The present interpretation of the experimental results differs from that of Mook and Shull[23] in that consistency with the s-d exchange Hamiltonian used here and other experimental information demands that the conduction-band spin density be

[31] J. C. Phillips and L. F. Mattheiss, Phys. Rev. Letters **11**, 556 (1963).
[32] J. C. Phillips, Phys. Rev. **133**, A1020 (1964).
[33] W. A. Harrison, Phys. Rev. **118**, 1182 (1960).
[34] G. C. Fletcher, Proc. Phys. Soc. (London) **A65**, 192 (1952).
[35] J. C. Slater and G. Koster, Phys. Rev. **94**, 1498 (1954).
[36] J. Friedel, P. Lenglart, and G. Leman, J. Phys. Chem. Solids **25**, 781 (1964); P. Lenglart, G. Leman, and J. P. Lelieur, *ibid.* **27**, 377 (1966).
[37] The usefulness of this point of view has been previously suggested by R. Nathans, S. J. Pickart, and H. A. Alperin, J. Phys. Soc. Japan **17**, Suppl. B-III, 7 (1962).
[38] B. W. Batterman, D. R. Chipman, and J. J. DeMarco, Phys. Rev. **122**, 68 (1961); L. D. Jennings, D. R. Chipman, and J. J. DeMarco, *ibid.* **135**, A1612 (1964).
[39] F. J. Arlinghaus, Ph.D. thesis, MIT, 1965 (unpublished).
[40] J. Friedel, J. Phys. Radium **16**, 829 (1955).
[41] A preliminary account of this work appears in L. Hodges, N. D. Lang, H. Ehrenreich, and A. J. Freeman, J. Appl. Phys. **37**, 1449 (1966).
[42] R. E. Watson and A. J. Freeman, Phys. Rev. **120**, 1125 (1960); **120**, 1134 (1960).
[43] The possible importance of this effect was suggested to us by A. J. Freeman (see Ref. 41).

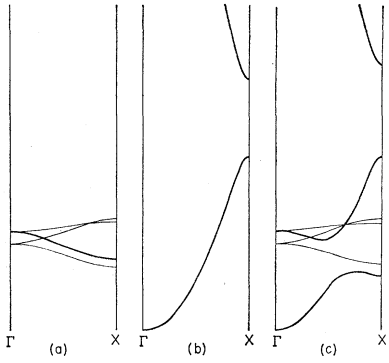

FIG. 1. Energy bands of an fcc transition metal along the [100] direction. The heavy bands all have Δ_1 symmetry and hybridize with each other. Panels (a) and (b) show d and conduction bands, respectively, before hybridization, and panel (c) shows the hybridized bands.

parallel to that of the d electrons near the cell origin and antiparallel near the boundary.[44] The admixture of T_{2g} and E_g orbitals giving rise to the observed asphericity of the spin density also differs from that deduced in the rather simpler analysis of Ref. 23. The agreement between theory and experiment, however, is substantially as good as that obtained in Ref. 23 except for the three lowest reflections. It is likely that an explanation of this discrepancy requires the use of first-principles unrestricted Hartree-Fock band wave functions for both d and conduction bands, since these points are importantly influenced by the contribution of paired electrons as well as that of certain s-d overlap and orthogonalization terms that are neglected in the present calculation.

II. INTERPOLATION SCHEMES

The interpolation scheme for the transition metals which will be discussed in the present section is based on the following ideas. First-principles calculations have shown that except for important hybridization effects, the d bands closely resemble those obtained in the tight-binding approximation, whereas the conduction bands are similar to those resulting from nearly-free-electron calculations. Accordingly, we shall represent the unhybridized d bands in terms of linear combinations of atomic orbitals[35] (LCAO), as in Fletcher's calculations for Ni,[34] and the conduction bands in terms of a four-OPW (orthogonalized-plane-wave) approximation, as in Harrison's calculations for Al.[33] Effects resulting from the hybridization of the conduction and d basis functions which are used here must be included separately.

These effects are illustrated in Fig. 1, which shows the paramagnetic energy bands of a typical fcc iron-group transition metal in the [100] direction. (These results actually correspond quantitatively to those for Cu.) The first panel shows the energy bands arising from the atomic d levels in the absence of conduction bands. The second panel shows the lowest conduction bands before hybridization with the d bands. The last panel illustrates the actual bands when hybridization effects are included. The heavily drawn bands all have the same Δ_1 symmetry and therefore hybridize.

Since the present interpolation scheme will be used to determine the band structure of ferromagnetic Ni, whose features depend essentially on the inclusion of electron correlation effects, it is necessary to consider an approximation to the full many-electron Hamiltonian more general than that of the usual one-electron Hartree-Fock scheme. We shall consider the Hamiltonian

$$H=H_{\text{band}}+H_{\text{so}}+H_{\text{corr}}, \tag{2.1}$$

in which the first term, to be discussed in Sec. IIA, gives the results of ordinary nonrelativistic band theory, the second, to be discussed in Sec. IIB, yields the effects of the spin-orbit interaction, and the third includes correlation effects in the approximation to be described in Sec. IIC.

The eigenvalue equation corresponding to H_{band} is

$$H_{\text{band}}B_{\mathbf{k}n}(\mathbf{r})=E_n(\mathbf{k})B_{\mathbf{k}n}(\mathbf{r}). \tag{2.2}$$

The Bloch eigenfunctions $B_{\mathbf{k}n}(\mathbf{r})$ are written as linear combinations of LCAO's $b_{\mathbf{k}\mu}(\mathbf{r})$ and OPW's $b_{\mathbf{k}\mathbf{K}}(\mathbf{r})$:

$$B_{\mathbf{k}n}(\mathbf{r})=\sum_\mu a_{n\mu}(\mathbf{k})b_{\mathbf{k}\mu}(\mathbf{r})+\sum_{\mathbf{K}} a_{n\mathbf{K}}(\mathbf{k})b_{\mathbf{k}\mathbf{K}}(\mathbf{r}). \tag{2.3}$$

The LCAO's are

$$\langle\mathbf{r}|\mathbf{k}\mu\rangle=b_{\mathbf{k}\mu}(\mathbf{r})=N^{-1/2}\sum_l e^{i\mathbf{k}\cdot\mathbf{R}_l}\varphi_\mu(\mathbf{r}-\mathbf{R}_l), \quad (\mu=1,\cdots,5), \tag{2.4}$$

where the $\varphi_\mu(\mathbf{r}-\mathbf{R}_l)$ are atomic d orbitals centered at the site $\mathbf{R}_l$, and N is the number of atoms in the solid. The OPW's have the form

$$\begin{aligned}\langle\mathbf{r}|\mathbf{k}+\mathbf{K},\, d\rangle&=b_{\mathbf{k}\mathbf{K}}(\mathbf{r})\\ &=\mathfrak{N}_{\mathbf{k}\mathbf{K}}^{-1/2}[\langle\mathbf{r}|\mathbf{k}+\mathbf{K}\rangle\\ &\quad-\sum_\mu\langle\mathbf{r}|\mathbf{k}\mu\rangle\langle\mathbf{k}\mu|\mathbf{k}+\mathbf{K}\rangle],\end{aligned} \tag{2.5}$$

where the $\mathbf{K}$ are reciprocal lattice vectors and the normalization factor is given by

$$\mathfrak{N}_{\mathbf{k}\mathbf{K}}=1-\sum_\mu|\langle\mathbf{k}\mu|\mathbf{k}+\mathbf{K}\rangle|^2. \tag{2.6}$$

The wave functions

$$\langle\mathbf{r}|\mathbf{k}+\mathbf{K}\rangle=(Nv_a)^{-1/2}e^{i(\mathbf{k}+\mathbf{K})\cdot\mathbf{r}} \tag{2.7}$$

are plane waves and v_a is the volume of the unit cell. The present scheme will use as basis functions the LCAO's defined in Eq. (2.4) and the plane waves given by Eq. (2.7) instead of the OPW's that are given in Eq. (2.5). Orthogonalization to core and d functions, which should in principle be included, will therefore not be considered explicitly here. It will be seen, nevertheless, that orthogonalization effects are taken into account approximately in the parametrized matrix elements of

[44] A. J. Freeman and R. E. Watson, in *Proceedings of the Second International Conference on the Mossbauer Effect, Saclay, France, 1961*, edited by A. H. Schoen and D. M. J. Compton (John Wiley & Sons, Inc., New York, 1962), p. 117.

the Hamiltonian. The eigenvector coefficients obtained in this scheme may then be identified directly with the a coefficients in Eq. (2.3). These points are discussed further in Sec. III.

The matrix elements of H_{band} will be expressed as $\mathbf{k}$-dependent terms multiplied by parameters representing various spatial integrals. These parameters are not actually determined from first principles, but are fit to give paramagnetic bands in agreement with the results of calculations done, for example, by the APW or Green's function methods. The correlation effects important in connection with ferromagnetism give rise to the Coulomb energy *change* that occurs when passing between the paramagnetic and ferromagnetic states. Instead of Eq. (2.1), it will therefore be more useful to consider

$$H=(H_{\text{band}}+H_{\text{corr}}{}^{\text{para}})+H_{\text{so}}+(H_{\text{corr}}{}^{\text{ferro}}-H_{\text{corr}}{}^{\text{para}}), \quad (2.8)$$

where the effective-band Hamiltonian $H_{\text{band}}{}^{\text{eff}}=H_{\text{band}}+H_{\text{corr}}{}^{\text{para}}$ will be assumed to include correlation effects associated with the paramagnetic state in some fashion. In practice, band calculations do not include these effects, but in view of their agreement with experiment, it is unlikely that the inclusion of correlation effects would produce major alterations in the quasiparticle energies. In the present paper the Coulomb interaction will be included in the manner proposed by Gutzwiller,[13] Hubbard,[14] and Kanamori.[15]

The spin-orbit interaction has been separated here from the other relativistic effects, which are not explicitly included, because it produces splittings in the band structure. The Darwin and mass-velocity terms produce only shifts and distortions in the band structure, and may therefore be regarded as being incorporated in H_{band}, at least in a qualitative way.

A. Interpolation Scheme: Cu and Paramagnetic Ni

As already noted, the basis set used in the present interpolation scheme consists of four OPW's (labeled by $\mathbf{K}$) representing the conduction bands in a nearly-free-electron approximation, and five LCAO's (indexed by $\mu=1,\cdots,5$) representing the $3d$ bands in a tight-binding approximation.

The appropriate OPW's for the 1/48 of the Brillouin zone in which $k_y\geq k_x\geq k_z\geq 0$ are formed from the plane waves $\langle\mathbf{r}|\mathbf{k}+\mathbf{K}\rangle$, where $\mathbf{K}_1=(0,0,0)$, $\mathbf{K}_2=(2\pi/a)(0,\bar{2},0)$, $\mathbf{K}_3=(2\pi/a)(\bar{1},\bar{1},\bar{1})$, and $\mathbf{K}_4=(2\pi/a)(\bar{1},\bar{1},1)$.

The LCAO's are given by Eq. (2.4). The atomic orbitals have the form

$$\begin{aligned}
\varphi_1(\mathbf{r})&=(15/4\pi)^{1/2}xy\,f^{T_{2g}}(r)/r^2,\\
\varphi_2(\mathbf{r})&=(15/4\pi)^{1/2}yz\,f^{T_{2g}}(r)/r^2,\\
\varphi_3(\mathbf{r})&=(15/4\pi)^{1/2}zx\,f^{T_{2g}}(r)/r^2,\\
\varphi_4(\mathbf{r})&=(15/16\pi)^{1/2}(x^2-y^2)f^{E_g}(r)/r^2,\\
\varphi_5(\mathbf{r})&=(5/16\pi)^{1/2}(3z^2-r^2)f^{E_g}(r)/r^2,
\end{aligned} \quad (2.9)$$

and satisfy $[(p^2/2m)+U(\mathbf{r})]\varphi(\mathbf{r})=E_{\text{atomic}}\varphi(\mathbf{r})$. Here $U(\mathbf{r})$ is the atomic potential and the $f^\mu(r)$ are the normalized radial functions of the isolated atom: $\int_0^\infty[rf^\mu(r)]^2dr=1$. As usual in the Slater-Koster interpolation scheme,[35] we shall neglect the nonorthogonality of the atomic orbitals associated with different sites.

The 18×18 matrix representing H_{band} may be written schematically as

$$[H_{\text{band}}]=\left(\begin{array}{cc|cc|cc}
s\uparrow\text{-}s\uparrow & & s\uparrow\text{-}d\uparrow & & & \\
 & & & & & \\
\hline
s\uparrow\text{-}d\uparrow & & d\uparrow\text{-}d\uparrow & & & \\
 & & & & & \\
\hline
 & & & & & \\
 & & & & & \\
 & & & & & \\
\end{array}\right.
\left.\begin{array}{cc|cc}
 & & & \\
 & & & \\
\hline
 & & & \\
 & & & \\
\hline
 & & s\downarrow\text{-}s\downarrow & s\downarrow\text{-}d\downarrow \\
 & & & \\
\hline
 & & s\downarrow\text{-}d\downarrow & d\downarrow\text{-}d\downarrow
\end{array}\right), \quad (2.10)$$

where s-s, d-d, and s-d refer, respectively, to the OPW, LCAO, and hybridization blocks. The energy eigenvalues are given by the solution of the secular equation

$$\det|\langle\mathbf{k}\nu\sigma|\,p^2/2m+V(\mathbf{r})\,|\mathbf{k}\nu'\sigma\rangle-E\langle\mathbf{k}\nu\sigma|\mathbf{k}\nu'\sigma\rangle|=0, \quad (2.11)$$

where ν includes the d and conduction band indices μ and $\mathbf{K}$. The presence of the factor $\langle\mathbf{k}\nu\sigma|\mathbf{k}\nu'\sigma\rangle$ indicates that the basis functions are not necessarily mutually orthogonal. This term appears most significantly in the hybridization block. In the paramagnetic case, the $\uparrow$-$\uparrow$ and $\downarrow$-$\downarrow$ blocks are identical, and only a 9×9 matrix need be considered in the actual calculations.

In Eq. (2.10), the matrix elements $H_{\mu\mu'}$ corresponding to the d-d block are given by

$$H_{\mu\mu'}=\langle\mathbf{k}\mu|\,p^2/2m+V(\mathbf{r})\,|\mathbf{k}\mu'\rangle.$$

If the crystal potential is written as a superposition of atomic potentials centered about sites $\mathbf{R}_l$,

$$V(\mathbf{r})=\textstyle\sum_l U(\mathbf{r}-\mathbf{R}_l), \quad (2.12)$$

we may use Eq. (2.4) to obtain

$$H_{\mu\mu'}=[E_0+\Delta(\delta_{\mu4}+\delta_{\mu5})]\delta_{\mu\mu'}+\sum_{l\neq0}e^{-i\mathbf{k}\cdot\mathbf{R}_l}\int\varphi_\mu{}^*(\mathbf{r}-\mathbf{R}_l)(V-U)\varphi_{\mu'}(\mathbf{r})d^3r, \quad (2.13)$$

where $\int\varphi_\mu{}^*(\mathbf{r})[p^2/2m+V(\mathbf{r})]\varphi_\mu(\mathbf{r})d^3r=E_0$ for $\mu=1,2,3$ and $E_0+\Delta$ for $\mu=4,5$. The energies E_0 and $E_0+\Delta$ are associated, respectively, with T_{2g} ($\mu=1,2,3$) and E_g ($\mu=4,5$) orbitals. Δ corresponds to the crystal-field splitting of the d bands at the point Γ. This procedure corresponds to Fletcher's approach, in which only terms corresponding to nearest-neighbor interactions were retained and the matrix elements $H_{\mu\mu'}$ were ex-

pressed in terms of six integrals $A_1,\cdots,A_6$ having the form

$$A_1=-\int \varphi_1^*(x-\tfrac{1}{2}a, y-\tfrac{1}{2}a, z)(V-U)\varphi_1(x,y,z)d^3r, \text{ etc.}$$

In the spirit of the Slater-Koster interpolation scheme,[35] these integrals are taken to be adjustable parameters, rather than being calculated from a model potential as in Fletcher's work.[34] In addition, E_0 and Δ are assumed adjustable. It should be noted that the actual splitting between Γ_{12} and Γ_{25}' is far larger than Δ because of the ligand-field effects arising from the A_i. In fact, in Fletcher's work, Δ was assumed to vanish. The present d-band interpolation scheme is useful because it has been shown to be applicable to a reasonable range of band widths.

The matrix elements $H_{\mathbf{K}\mathbf{K}'}$ corresponding to the s-s block have the form

$$[H_{\mathbf{K}\mathbf{K}'}]=\begin{bmatrix} \beta+\alpha|\mathbf{k}|^2 & V_{200}F_{0\bar{2}0} & V_{111}F_{\bar{1}\bar{1}\bar{1}} & V_{111}F_{\bar{1}\bar{1}1} \\ V_{200}F_{0\bar{2}0} & \beta+\alpha|\mathbf{k}+\mathbf{K}_2|^2 & V_{111}F_{0\bar{2}0}F_{\bar{1}\bar{1}\bar{1}} & V_{111}F_{0\bar{2}0}F_{\bar{1}\bar{1}1} \\ V_{111}F_{\bar{1}\bar{1}\bar{1}} & V_{111}F_{0\bar{2}0}F_{\bar{1}\bar{1}\bar{1}} & \beta+\alpha|\mathbf{k}+\mathbf{K}_3|^2 & V_{200}F_{\bar{1}\bar{1}\bar{1}}F_{\bar{1}\bar{1}1} \\ V_{111}F_{\bar{1}\bar{1}1} & V_{111}F_{0\bar{2}0}F_{\bar{1}\bar{1}1} & V_{200}F_{\bar{1}\bar{1}\bar{1}}F_{\bar{1}\bar{1}1} & \beta+\alpha|\mathbf{k}+\mathbf{K}_4|^2 \end{bmatrix}, \tag{2.14}$$

where F_{000}, which appears in all terms of the matrix containing only a single F, is unity and has been suppressed. With the exception of the appearance of the factors F, to be discussed below, this matrix is the same as that used in Harrison's treatment[33] of the conduction bands of Al. The diagonal matrix elements correspond to a band having a simple parabolic form; β is a constant fixing the zero of energy. The real crystal potential, as well as orthogonalization effects, are represented by a pseudopotential $V_p(\mathbf{r})=\sum_{\mathbf{K}} V_{\mathbf{K}}e^{i\mathbf{K}\cdot\mathbf{r}}$. In the transition metals, the first two Fourier coefficients, V_{111} and V_{200}, have values which are larger than in Al, corresponding to the fact that the splittings at the zone faces are larger. Mueller[27] has shown that these splittings arise from the d-function admixture into the conduction-band wave functions resulting from orthogonalization effects. Our parametrization of the problem differs from that of Ref. 27 in that the large conduction-band splittings are incorporated directly in the parameters α, V_{111}, V_{200}. The relation of our scheme to that of Mueller is established in Sec. III.

Because of the larger $V_{\mathbf{K}}$ relative to the polyvalent metals, it is necessary to ensure the occurrence of properly symmetrized combinations of OPW's along symmetry directions. Accordingly, one modifies the OPW matrix elements for the case of the fcc lattice by introducing symmetrizing factors $F_{0\bar{2}0}(\mathbf{k})$, $F_{\bar{1}\bar{1}\bar{1}}(\mathbf{k})$, and $F_{\bar{1}\bar{1}1}(\mathbf{k})$. The omission of these factors would result in small but undesirable energy splittings and shifts of the order of the average deviation of the interpolated bands from those of first-principles calculations. The F's should have the values given in Table I at symmetry points, and should vary smoothly in between.

TABLE I. Values of the symmetrizing factors at symmetry points.

	$F_{0\bar{2}0}$	$F_{\bar{1}\bar{1}\bar{1}}$	$F_{\bar{1}\bar{1}1}$
$\Gamma(000)$	0	0	0
$X(080)$	1	0	0
$L(444)$	0	1	0
$K(660)$	0	1	1
$W(480)$	1	1	1
$U(282)$	1	1	0

According to Eq. (2.11), the off-diagonal elements of the secular matrix between PW's and LCAO's are

$$(H-E)_{\mathbf{K}\mu}=\langle\mathbf{k}+\mathbf{K}|\,p^2/2m+V(\mathbf{r})\,|\mathbf{k}\mu\rangle -E\langle\mathbf{k}+\mathbf{K}|\mathbf{k}\mu\rangle. \tag{2.15}$$

It is necessary to make several approximations to reduce these matrix elements to an easily parametrized form. Expressing $V(\mathbf{r})$ in terms of atomic potentials [Eq. (2.12)], and $|\mathbf{k}\mu\rangle$ in terms of LCAO's [Eq. (2.4)], we obtain, using (2.7),

$$(H-E)_{\mathbf{K}\mu}=(v_a)^{-1/2}\int e^{-i(\mathbf{k}+\mathbf{K})\cdot\mathbf{r}}\sum_{l\neq 0} U(\mathbf{r}-\mathbf{R}_l)\varphi_\mu(\mathbf{r})d^3r - (E-E_{\text{at.}})(v_a)^{-1/2}\int e^{-i(\mathbf{k}+\mathbf{K})\cdot\mathbf{r}}\varphi_\mu(\mathbf{r})d^3r. \tag{2.16}$$

The first term may be written in a simpler parametrized form if it is assumed that the main contribution to the integral comes from the region (near a cell boundary) of maximum overlap between potential and wave function, where U should be relatively slowly varying. Hence, $\sum_{l\neq 0} U(\mathbf{r}-\mathbf{R}_l)$ in Eq. (2.16) will be approximated by a constant $\bar{U}$. In the second term, it will be assumed that E can be replaced by an average value $\bar{E}$. It should be recalled that this term would have been unnecessary if properly d-orthogonalized conduction-band wave functions had been used. The replacement of E by $\bar{E}$ is equivalent to the use of an approximately orthogonal basis and is found to be entirely satisfactory if the range of energies under consideration is not too large. Equation (2.16) then simplifies considerably:

$$(H-E)_{\mathbf{K}\mu}=(\bar{U}-\bar{E}+E_{\text{at.}})(v_a)^{-1/2} \times\int e^{-i(\mathbf{k}+\mathbf{K})\cdot\mathbf{r}}\varphi_\mu(\mathbf{r})d^3r. \tag{2.17}$$

By expanding the exponential factor in spherical harmonics ans spherical Bessel functions, and by noting

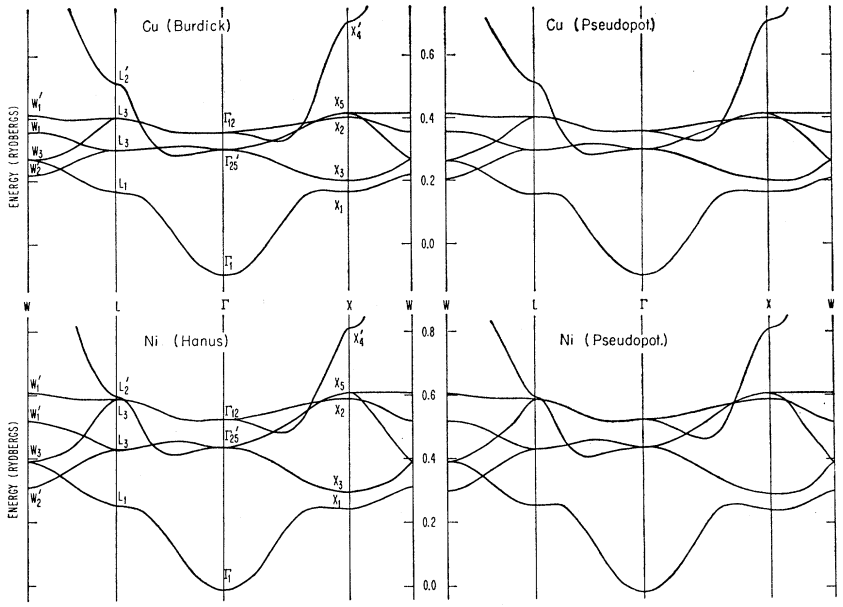

FIG. 2. Comparison along selected symmetry lines of energy bands calculated by the APW method for Cu by Burdick (Ref. 4) and for paramagnetic Ni by Hanus (Ref. 5) with the interpolated bands of the present scheme.

that only the term $l=2$ contributes to the integral, we may reduce the radial part to the parametrized form $\int_0^\infty j_2(kr)r^2f(r)dr \propto j_2(kB_1)$, where the integral has been evaluated on the assumption that $r^2f(r)$ is strongly peaked at B_1. The constant factors proportional to $(\bar{U}-\bar{E}+E_{\text{at.}})$ are combined into another adjustable constant B_2. The final parametrized result including the symmetrizing factors $F_{\mathbf{K}}(\mathbf{k})$ (with $F_{000}\equiv 1$) is

$$
\begin{aligned}
(H-E)_{\mathbf{K}i} &= B_2 j_2(|\mathbf{k}+\mathbf{K}|B_1) \\
&\quad \times\left[\frac{(\mathbf{k}+\mathbf{K})_\mu(\mathbf{k}+\mathbf{K})_\nu}{|\mathbf{k}+\mathbf{K}|^2}\right]F_{\mathbf{K}}(\mathbf{k}), \\
&\quad (i,\mu,\nu)=(1,x,y),\ (2,y,z),\ (3,z,x), \\
(H-E)_{\mathbf{K}4} &= B_2 j_2(|\mathbf{k}+\mathbf{K}|B_1) \\
&\quad \times\frac{(\mathbf{k}+\mathbf{K})_x^2-(\mathbf{k}+\mathbf{K})_y^2}{2|\mathbf{k}+\mathbf{K}|^2}F_{\mathbf{K}}(\mathbf{k}), \\
(H-E)_{\mathbf{K}5} &= B_2 j_2(|\mathbf{k}+\mathbf{K}|B_1) \\
&\quad \times\tfrac{1}{6}\sqrt{3}\left[\frac{3(\mathbf{k}+\mathbf{K})_z^2}{|\mathbf{k}+\mathbf{K}|^2}-1\right]F_{\mathbf{K}}(\mathbf{k}).
\end{aligned}
\tag{2.18}
$$

While these approximations would not be expected to yield reliable results if the parameters B_1 and B_2 appearing in the preceding equations were calculated from first principles, they do lead to a reasonable representation of the band structure provided that they are regarded as adjustable.

Equations (2.18) are a severely approximated version of the original Eqs. (2.15). However, they contain all the essential physical ingredients associated with hybridization and nonorthogonality, at least in an approximate way, and will be seen to yield excellent results.

The parameters appearing in our scheme are chosen by fitting the pseudopotential bands at symmetry points to accurately calculated bands. The parameters $A_1, \cdots, A_6$, E_0, and Δ are evaluated from pure d levels at Γ, L, X, and K, where the Hamiltonian matrix is very simple. The parameter β is the energy of the lowest-lying pure conduction level at Γ_1. The remaining parameters α, V_{111}, and V_{200} are fitted to points sufficiently high in the conduction bands that hybridization with d levels no longer plays a significant role. B_1 and B_2 are chosen to give the correct hybridization at L and X: of course, other symmetry points may be used instead. We have actually used the same value of B_1 for both Cu and Ni. This simplified form of the hybridization is found to give very good results at all points of the Brillouin zone.

Figure 2 shows the agreement between the pseudopotential interpolation scheme and APW calculations for Cu (Burdick[4]) and Ni (Hanus[5]). The excellence of the fit is characterized by the following deviations from the APW bands calculated at 89 points in 1/48 of the Brillouin zone in Cu and 28 points in Ni. The average, root-mean-square, and maximum deviations are respectively 0.09, 0.11, and 0.37 eV for Cu and 0.09, 0.13, and 0.42 eV for Ni.

Calculations with this interpolation scheme can be carried out rapidly on a computer: less than a minute of IBM 7094 time is required to calculate the matrix elements, eigenvalues, and eigenvectors at 89 points in the Brillouin zone, as well as the density of states, using routine matrix diagonalization methods.

B. Spin-Orbit Effects

The spin-orbit interaction can be written in the Hartree approximation as

$$H_{\text{SO}}=(\hbar/4m^2c^2)\boldsymbol{\sigma}\cdot\nabla V\times\mathbf{p},$$

where V is the crystal potential. The principal qualita-

tive effect of this interaction is to produce additional splittings in the d bands. The remaining effects are purely quantitative. They result in shifts and distortions of the bands which, in the context of the present interpolation scheme, can be assumed to be incorporated in the parameters discussed in Sec. IIA. Accordingly, it is reasonable to include in the matrix representation of H_{so} only elements between d functions, and to neglect matrix elements between two conduction-band functions, and between conduction-band and d functions. In effect, therefore, spin-orbit-split d bands are hybridized with the conduction bands of Sec. IIA. The preceding approximation has the convenience that the elements of the matrix for H_{so} worked out by Friedel, Lenglart, and Leman[36] for d bands in the tight-binding approximation can be immediately used.

If the crystal potential is written as a superposition of atomic potentials as in Eq. (2.12), then the spin-orbit interaction among d electrons can be written is second-quantized notation as

$$H_{so}=\sum_{\substack{i\mu\mu'\\ \sigma\sigma'}} c_{i\mu\sigma}{}^{\dagger}c_{i\mu'\sigma'}\langle\mu\sigma|\,\xi(r)\mathbf{L}\cdot\mathbf{S}\,|\mu'\sigma'\rangle\,, \qquad (2.19)$$

where $\xi(r)=(\hbar^2/2m^2c^2r)dU/dr$, only intra-atomic terms are retained, and $U(r)$ is taken to be spherically symmetric. Here $|\mu\sigma\rangle,|\mu'\sigma'\rangle$ refer to orbitals centered about the origin. The matrix elements $\langle\mu\sigma|\,\xi(r)\mathbf{L}\cdot\mathbf{S}\,|\mu'\sigma'\rangle$ are proportional to the spin-orbit parameter $\zeta=\int_0^\infty[rf(r)]^2\times\xi(r)dr$, where $f(r)$ is defined in Eq. (2.9). In connection with the present interpolation scheme, ζ is properly regarded as another adjustable constant, not necessarily equal to the atomic value.

The 18×18 matrix that replaces that of Eq. (2.10) can be written schematically as

$$[H_{\text{band}}]+\left(\begin{array}{c|c|c|c} 0 & 0 & 0 & 0 \\ \hline 0 & d\uparrow\text{-}d\uparrow & 0 & d\uparrow\text{-}d\downarrow \\ \hline 0 & 0 & 0 & 0 \\ \hline 0 & d\downarrow\text{-}d\uparrow & 0 & d\downarrow\text{-}d\downarrow \end{array}\right), \qquad (2.20)$$

where the right-hand term represents the effects of spin-orbit coupling in our approximation.

In the present applications of this formalism, we shall examine the effects of spin-orbit interactions on purely nonrelativistic band structures instead of fitting the entire Hamiltonian $H_{\text{band}}+H_{so}$ to a first-principles calculation including spin-orbit splitting. While realizing that the approximation may be quantitatively inadequate, we shall regard the parameter ζ to be given by its atomic value, determined from spectroscopic data, instead of by the best possible fit to a band calculation. In this connection it should be noted that even though the magnitude of the spin-orbit interaction is determined near the core where the potential is atomic-like, the effects of the solid are not negligible.

C. Correlation Effects

The pseudopotential method developed in Sec. II.A can be used to infer fairly realistically features of the band structure of magnetic materials like Ni. As we shall see from the particular example to be considered here, such calculations always involve a self-consistency condition, since the spin polarization of a given electron will depend in some manner on that of all the other electrons. While self-consistency procedures have, until the present time, been prohibitive for first-principles band calculations as complicated as those encountered in the $3d$ metals, they are quite feasible in connection with pseudopotential techniques. In addition, the motivation for embarking upon first-principles calculations is less compelling, since the Hamiltonian to be considered in connection with the magnetic properties should in principle contain the full Coulomb interaction. Tractable interaction terms, of course, require gross simplification.

One particularly simple version of the interaction Hamiltonian, a generalization of that originally proposed by Gutzwiller,[13] Hubbard,[14] and Kanamori,[15] and recently discussed in detail by Herring,[1] has the form

$$H_{\text{corr}}=U^{d\text{-}d}\sum_{i\mu}n_{i\mu\uparrow}n_{i\mu\downarrow}+U'^{d\text{-}d}\sum_{\substack{i\sigma\sigma'\\ \mu\neq\mu'}}n_{i\mu\sigma}n_{i\mu'\sigma'}$$
$$-J^{d\text{-}d}\sum_{\substack{i\sigma\\ \mu\neq\mu'}}n_{i\mu\sigma}n_{i\mu'\sigma}-J^{s\text{-}d}\sum_{i\sigma\mathbf{K}\mu}n_{i\mu\sigma}n_{i\mathbf{K}\sigma}\,, \qquad (2.21)$$

where σ,σ' are spin indices. The first term describes the intra-atomic Coulomb repulsion between two antiparallel d electrons in the same orbital μ on the same atom at site i, and the second term describes the Coulomb repulsion between d electrons in different orbitals on the same atom.

$$U^{d\text{-}d}=\int\varphi_\mu{}^*(\mathbf{r}_1)\varphi_\mu{}^*(\mathbf{r}_2)e^2|\,\mathbf{r}_1-\mathbf{r}_2\,|^{-1}\varphi_\mu(\mathbf{r}_2)\varphi_\mu(\mathbf{r}_1)d^3r_1d^3r_2$$

and $U'^{d\text{-}d}$, correspondingly defined, are the respective polarity energies. It should be noted that Eq. (2.21) assumes the same value of $U'^{d\text{-}d}$ independently of the relative electron spins in the two orbitals. The third and fourth terms correspond, respectively, to exchange interactions among d orbitals and between d and s orbitals. We neglect the magnetic effects of s-s exchange interactions and assume the polarization of the conduction electrons to arise purely from the magnetization of the d electrons via a Hund's-rule coupling ($J^{s\text{-}d}$).

Since we are interested in the application of this Hamiltonian to the problem of ferromagnetism, we shall retain only those terms which produce an energy change when passing between the paramagnetic and ferromagnetic states. We shall perform the separation indicated in Eq. (2.8), assuming the band Hamiltonian to include paramagnetic correlation effects, and con-

sidering the correlation Hamiltonian to be given by $H_{\text{corr}}^{\text{ferro}}-H_{\text{corr}}^{\text{para}}$. We can effect further simplification with the help of Herring's estimates of the parameters appearing in Eq. (2.21). He finds $U^{d\text{-}d}\approx 5$ eV, $U'^{d\text{-}d}\approx 3$ eV, $J^{d\text{-}d}\approx 1$ eV. Thus $J^{d\text{-}d}$ is seen to be rather smaller than $U'^{d\text{-}d}$. We accordingly neglect this term, even though Herring has pointed out that since its contribution to the magnetization energy is of the order of $K\Theta_c$, where Θ_c is the Curie temperature, it may be crucial to the appearance of ferromagnetism in Ni. Within the context of an interpolation scheme in which the effective polarity and exchange energies are considered to be adjustable parameters (see below), rather than being calculated from first principles, such an approach is justified, since the physical effect of the terms in $U^{d\text{-}d}$ and $J^{d\text{-}d}$ is actually the same: Both result in a decrease of energy when passing from the paramagnetic to the ferromagnetic state.

Actually, due to correlations among itinerant electrons, the real polarity energy $U^{d\text{-}d}$ is reduced to an effective polarity energy $U_{\text{eff}}^{d\text{-}d}$. This effect owes its existence to the fact that electrons have a choice of either going onto sites that already contain an antiparallel-spin electron in the same orbital, or avoiding such sites. The latter choice implies that part of the crystal volume is unavailable to the electrons and results in an increase of the kinetic energy. As shown by Kanamori[15] and Herring,[1] a consequence of this fact is that $U_{\text{eff}}^{d\text{-}d}$ can never exceed the band width, even though $U^{d\text{-}d}$ may be very large. A similar reduction of the exchange energy $J^{s\text{-}d}$ to an effective value $J_{\text{eff}}^{s\text{-}d}$ will also occur. The calculation of the effective polarity and exchange energies has been carried out by Kanamori using an adaptation of the Brueckner-Goldstone method, in which the interaction is replaced by a sum of ladder diagrams. This method is expected to be valid when the potential is short-ranged or the density of particles is low, i.e., when $ak_F\ll 1$, where a is the range of the potential and k_F is the Fermi wave number. If we consider the simplest model of Ni, in which one assumes equal numbers of holes in the d band near X_5 and electrons in the conduction band, equal to 0.6 per atom, then ak_F is not small if a is taken to be the Thomas-Fermi length which is determined by the screening due to the conduction electrons. However, k_F is reduced due to the fact that the top of the d band (X_5) consists of three-fold-degenerate T_{2g} orbitals. Even under these conditions, $ak_F\approx 0.4$. Accordingly, this treatment of strong correlations may not be quantitatively valid. However, in view of the fact that $U_{\text{eff}}^{d\text{-}d}$ and $J_{\text{eff}}^{s\text{-}d}$ represent adjustable parameters, our resultant effective Hamiltonian may be considered to be an adequate starting point.

While Kanamori considered in detail only the case of a single nondegenerate band, Herring generalized his treatment to include three-fold degeneracy, corresponding to the holes in the d bands near the X_5 level. Herring's treatment may be easily generalized further to apply to the present more complicated situation. Similar results are obtained: When $U'^{d\text{-}d}\gg J^{d\text{-}d}$, the terms involving these quantities make a negligible contribution to $H_{\text{corr}}^{\text{ferro}}-H_{\text{corr}}^{\text{para}}$ since the term involving $U'^{d\text{-}d}$ is independent of the relative spins of the electrons in the two orbitals involved, and there is almost no preferential alignment provided by the exchange interaction because of its small magnitude. The only significant terms remainin in H_{corr}, then, are those involving $U_{\text{eff}}^{d\text{-}d}$ and $J_{\text{eff}}^{s\text{-}d}$.

Within the context of Herring's treatment, the assumed $\mathbf{k}$ independence of $U^{d\text{-}d}$ and $J^{s\text{-}d}$ implies that $U_{\text{eff}}^{d\text{-}d}$ and $J_{\text{eff}}^{s\text{-}d}$ are also constant. While such an assumption may be physically reasonable for $U_{\text{eff}}^{d\text{-}d}$, it is rather crude for $J_{\text{eff}}^{s\text{-}d}$, as we shall discuss later in Sec. V.

One further approximation is required in order to obtain a tractable expression. After replacing the strong interactions by weaker effective interactions with the help of t-matrix techniques, it is reasonable to treat this residual interaction in terms of the Hartree-Fock approximation. The effective interaction Hamiltonian then becomes

$$H_{\text{corr}}=U_{\text{eff}}^{d\text{-}d}\sum_{i\mu\sigma}n_{i\mu\sigma}[\langle n_{i\mu,-\sigma}\rangle^{\text{ferro}}-\langle n_{i\mu,-\sigma}\rangle^{\text{para}}]$$
$$-J_{\text{eff}}^{s\text{-}d}\sum_{i\mu\mathbf{K}\sigma}n_{i\mathbf{K}\sigma}[\langle n_{i\mu\sigma}\rangle^{\text{ferro}}-\langle n_{i\mu\sigma}\rangle^{\text{para}}]. \quad (2.22)$$

The form of Eq. (2.22) assumes that the magnetization of conduction electrons is determined by d electrons, and that the effect of the conduction-electron polarization on d electrons is negligible compared to that of the d electrons on each other. In considerations involving only ferromagnetic ordering, it is sufficient to consider only the spatially homogeneous expectation value[14] $\langle n_{i\mu\sigma}\rangle=\langle n_{\mu\sigma}\rangle=N^{-1}\sum_{n\mathbf{k}\text{ occ}}|a_{n\mu\sigma}(\mathbf{k})|^2$, in terms of the a coefficients defined in Eq. (2.3).

The Hamiltonian (2.22) may then be transformed into $\mathbf{k}$ space to give

$$H_{\text{corr}}=U_{\text{eff}}^{d\text{-}d}\sum_{\mathbf{k}\mu\sigma}n_{\mathbf{k}\mu\sigma}[\langle n_{\mu,-\sigma}\rangle^{\text{ferro}}-\langle n_{\mu,-\sigma}\rangle^{\text{para}}]$$
$$-J_{\text{eff}}^{s\text{-}d}\sum_{\mathbf{k}\mathbf{K}\mu\sigma}n_{\mathbf{k}\mathbf{K}\sigma}[\langle n_{\mu\sigma}\rangle^{\text{ferro}}-\langle n_{\mu\sigma}\rangle^{\text{para}}]. \quad (2.23)$$

H_{corr} has diagonal form, and modifies the band Hamiltonian [Eq. (2.10)] in the following manner. The diagonal conduction-band components of spin σ and diagonal d components of orbital μ and spin σ are altered by the addition of the energies

$$-J_{\text{eff}}^{s\text{-}d}\sum_{\mu}[\langle n_{\mu\sigma}\rangle^{\text{ferro}}-\langle n_{\mu\sigma}\rangle^{\text{para}}]$$

and

$$U_{\text{eff}}^{d\text{-}d}[\langle n_{\mu,-\sigma}\rangle^{\text{ferro}}-\langle n_{\mu,-\sigma}\rangle^{\text{para}}],$$

respectively. Since the d wave functions in a cubic field decompose into T_{2g} ($\mu=1,2,3$) and E_g ($\mu=4,5$) orbitals, we find $\langle n_{1\sigma}\rangle=\langle n_{2\sigma}\rangle=\langle n_{3\sigma}\rangle$ and $\langle n_{4\sigma}\rangle=\langle n_{5\sigma}\rangle$. Thus at points of the Brillouin zone where the wave functions have pure T_{2g} (e.g., W_1', X_5, X_3, Γ_{25}') or E_g (e.g., X_2, Γ_{12}, K_4) symmetry, the d part of the Hamiltonian matrix is diagonal and the splitting among such levels is rigid. However, because the population of T_{2g} and E_g

levels is affected differently in going from the paramagnetic to the ferromagnetic state, the form of H_{corr} in Eq. (2.23) predicts that the splitting of pure T_{2g} and E_g levels should differ. At general points of the Brillouin zone, where the wave function involves a $\mathbf{k}$-dependent linear combination of both types of orbitals, the splitting will therefore also be $\mathbf{k}$ dependent. This behavior contrasts with previously used, simpler, model Hamiltonians which assumed the d-band splitting to be rigid. It should be emphasized that further $\mathbf{k}$ dependence would be introduced if $U_{\text{eff}}^{d\text{-}d}$ were properly regarded as $\mathbf{k}$ dependent and if the d bands were described in an approximation that went beyond that used here.

As already pointed out, $U_{\text{eff}}^{d\text{-}d}$ and $J_{\text{eff}}^{s\text{-}d}$ are treated as adjustable parameters in the present interpolation scheme, and are chosen in a manner to be discussed later to fit experimental data such as the magneton number. The general procedure for obtaining a ferromagnetic electron band structure, then, is the following. One begins by fitting to a band calculation for the paramagnetic state and thereby fixes all parameters except $U_{\text{eff}}^{d\text{-}d}$ and $J_{\text{eff}}^{s\text{-}d}$, which are specifically associated with the ferromagnetic state. In passing to the ferromagnetic state the parameters characterizing the paramagnetic band structures are not adjusted further, or at most adjusted slightly. The introduction of H_{corr} involves a self-consistency condition: The band structure appropriate to a given $U_{\text{eff}}^{d\text{-}d}$ and $J_{\text{eff}}^{s\text{-}d}$ must yield the same values of $\langle n_{\mu\sigma}\rangle^{\text{ferro}}-\langle n_{\mu\sigma}\rangle^{\text{para}}$ as those used in the input. In order to obtain agreement with the magneton number and related physical quantities, it is perhaps simplest to obtain self-consistent solutions of the problem for several $U_{\text{eff}}^{d\text{-}d}$ and $J_{\text{eff}}^{s\text{-}d}$ and then by interpolation to determine the values most nearly consistent with experimental observations.

III. SIGNIFICANCE OF INTERPOLATION ENERGY BANDS AND WAVE FUNCTIONS

Interpolation schemes such as that described in Sec. II represent electronic energy bands in terms of a few adjustable parameters. Once the energy eigenvalues have been obtained from the solution of the secular equation (2.11), it is a simple matter to evaluate the eigenvector coefficients. In order to obtain the pseudopotential wave functions for the solid, these coefficients must be associated with the proper basis functions.

In Sec. II.A, the parametrized form of the Hamiltonian matrix was derived using a nonorthogonal basis composed of LCAO's [Eq. (2.4)] and plane waves [Eq. (2.7)]. However, with the help of the approximations to be discussed below, one can show that the use of an orthogonal basis of LCAO's and OPW's [Eq. (2.5)] leads to exactly the same parametrized form of the Hamiltonian matrix, where, indeed, the new parameters are differently defined. However, in view of the fact that their numerical values are chosen to reproduce the actual band structure, this difference is without significance in the context of an interpolation scheme. The adjustable parameters in fact implicitly include effects associated with an orthogonal basis, and in particular, the large conduction-band orthogonalization shifts discussed by Mueller.[27] By the same argument, the eigenvector coefficients will also be seen to be associated, to a good approximation, with OPW's and LCAO's.

These points may be justified by considering explicitly the Hamiltonian in the context of the basis set of OPW's and LCAO's. This basis is orthogonal except for a slight nonorthogonality of the OPW's among themselves, which may be neglected. The various matrix elements of the Hamiltonian may be computed using the procedures employed in Sec. IIA. The d-d matrix elements are identical to those of Eq. (2.13). The s-d hybridization matrix elements are identical to those of Eq. (2.18) if the parameter B_2 is reinterpreted to be proportional to $\bar{U}$ rather than to $\bar{U}-\bar{E}+E_{\text{at.}}$.

Significant changes, however, occur in the s-s block. The diagonal matrix elements replacing those in Eq. (2.14) do not have a simple parabolic form, nor are the off-diagonal elements simply equal to the pseudopotential parameters V_{111} and V_{200}. All elements in the s-s block now include complicated terms involving normalization factors such as those in Eq. (2.6), orthogonality integrals of the form $\langle \mathbf{k}\mu|\mathbf{k}+\mathbf{K}\rangle$, hybridization integrals between plane waves and LCAO's similar to those in Eq. (2.18), and matrix elements similar to those appearing in Eq. (2.13). A natural approximation to make at this point is to neglect the $\mathbf{k}$ dependence of these terms and to group them together into new constants. The resulting matrix is then identical to that of Sec. IIA, which was derived using the nonorthogonal basis. This approximation is the same as that employed by Harrison,[33] who also found it unnecessary to include explicit core orthogonalization in his 4-OPW interpolation scheme for Al. In fact, however, orthogonality effects are neither neglected in Harrison's work nor in the present calculations, since the parameters α, V_{111}, and V_{200} include these effects in an approximate way. Since the d bands are, in the case of the transition metals, not part of the core, the explicit neglect of s-d orthogonalization may be viewed as a much more serious approximation. However, in view of the excellent results achieved by the present interpolation scheme, it is clear that the simplified treatment of these terms is entirely adequate. The interpolation scheme of Mueller[27] differs essentially from the present one only in the retention of these complicated terms, since the d-d and s-d blocks in his scheme are very similar to those of the present work.

In order to make these points more explicit, let us consider the special case of the conduction bands at L_2' and L_1. The L_2' wave function is automatically orthogonal to all of the d-band LCAO's and does not hybridize with any of them. The energy of the L_1 level, however, does include shifts due to orthogonalization

and hybridization, as Mueller[27] has pointed out. If we represent these energy shifts by E_{hyb} and E_{orth}, the energies of the L_1 and L_2' levels may be written as

$$E(L_1)=\beta+48\alpha'+V_{111}'+E_{\text{hyb}}+E_{\text{orth}},$$
$$E(L_2')=\beta+48\alpha'-V_{111}', \tag{3.1}$$

in terms of parameters α' and V_{111}' characteristic of an interpolation scheme, such as Mueller's, which retains orthogonalization terms. Equations (3.1) may be used to fit the parameters α' and V_{111}'. In the present simplified scheme, however, the appropriate equations are

$$E(L_1)=\beta+48\alpha+V_{111}+E_{\text{hyb}},$$
$$E(L_2')=\beta+48\alpha-V_{111}, \tag{3.2}$$

which may also be fit by an appropriate choice of α and V_{111}. Explicit comparison of Eqs. (3.1) and (3.2) shows that the unprimed parameters are larger than the primed ones, and hence that they include orthogonalization effects approximately. An argument similar to the one made here for L applies to other points in the Brillouin zone as well. As a result, the parameters α, V_{111}, and V_{200} have different values at different points in $\mathbf{k}$ space. As already pointed out, this $\mathbf{k}$ dependence is relatively unimportant if attention is restricted to a finite energy range. A single set of values of these parameters has indeed been found to yield energy bands of Cu and Ni in good agreement with first-principles calculations for a range of energies extending from the bottom of the conduction band to several volts above the Fermi level. The preceding line of argument may be immediately extended to the eigenvector coefficients $a_{n\mathbf{K}}(\mathbf{k})$ and $a_{n\mu}(\mathbf{k})$, which, accordingly, may be associated with the true conduction and d-band wave functions, respectively. However, it is still necessary to verify in some detail that these lead to physically reasonable results by examining the actual spatial dependence of the Bloch functions of Eq. (2.3).

In the spirit of the present interpolation scheme, one would suppose that if the pseudopotential wave functions agreed with the wave functions obtained from first-principles calculations at a representative set of points in the Brillouin zone, then they would be significant throughout most of the zone. It should be noted, of course, that the physical significance of these wave functions would certainly be no greater than that of the results from first principles, which are often of doubtful validity.

In the noble and transition metals, APW calculations have indicated that the wave functions near the top of the d bands are well represented by LCAO's constructed from atomic functions.[7] At lower d-band energies, however, the deviations from atomic character become relatively pronounced, since the APW wave functions are more spread out over the unit cell. The basis functions used in connection with the present pseudopotential interpolation scheme therefore insure that

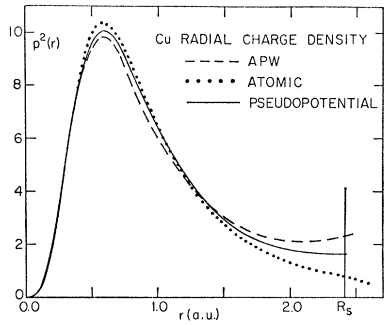

FIG. 3. The radial charge density in Cu computed, respectively, from APW calculations by Arlinghaus (Ref. 39), the atomic calculations of Herman and Skillman (Ref. 45), and the present pseudopotential scheme. R_s is half the nearest-neighbor distance, or the radius of the APW sphere. (a.u.=atomic units).

the d components of the wave functions are reasonably good near the top of the d bands. At lower d-band energies, one would hope that the parametrized hybridization effects with conduction-band wave functions might correspond in some reasonable manner to the delocalization of the d functions and their deviation from atomic character. It should be emphasized that the full description of this effect would almost certainly require a variation of $f(r)$ in Eq. (2.9) with d-band energy. We shall not, however, consider this energy dependence of $f(r)$, since the neutron-diffraction results for which the pseudopotential wave functions will be used most extensively are determined by electrons near the top of the d band.

In fact, however, it appears that even the crude wave functions obtained from Eq. (2.3) are adequate to give a reasonable representation of the total charge density in the solid. The results for Cu may be considered in this connection. Arlinghaus[39] has calculated the radial charge density and x-ray form factor in Cu using the wave functions obtained from an APW calculation of the band structure. The x-ray form factor calculated in this way agrees with experiment much better than the atomic form factor, because of the spreading out of the copper valence-electron charge density in passing from the atom to the solid.

The charge density calculated in Ref. 39 is compared in Fig. 3 with the charge density obtained from the present interpolation scheme using the atomic $3d$ functions of Herman and Skillman[45] to determine $f(r)$. The agreement between the two sets of results is seen to be quite good. The largest discrepancy occurs in the outer parts of the unit cell where the d functions near the bottom of the bands make the dominant contribution. As expected, the present interpolation scheme does not represent the delocalized functions as well as it does the wave functions associated with the top of the d-band complex. The figure also shows the atomic charge density computed from the atomic $3d$ and $4s$ functions

[45] F. Herman and S. Skillman, *Atomic Structure Calculations* (Prentice-Hall, Inc., Englewood Cliffs, New Jersey, 1963).

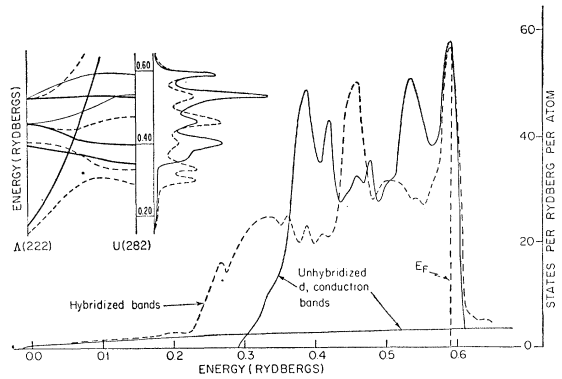

FIG. 4. The density of states of paramagnetic Ni for the hybridized bands and the unhybridized d and conduction bands. The inset shows the energy bands and density of states along the line from $\Lambda(222)$ to $U(282)$ both before (solid lines) and after (dashed and light solid lines) hybridization; the light solid lines correspond to nonhybridizing bands.

of Herman and Skillman. While qualitatively similar to the "band" charge density, the atomic density is seen to be somewhat less diffuse. The good agreement between the two calculated total charge densities provides some confidence in the validity of the neutron-diffraction calculations of Sec. VI, in which the net spin density, and hence the wave functions, is needed to calculate the magnetic form factor. This is true particularly in view of the already mentioned fact that the net spin density is determined largely by electrons near the top of the d band, rather than by electrons throughout the entire band structure which must be considered in connection with the total charge density.

IV. HYBRIDIZATION, SPIN-ORBIT EFFECTS, DENSITY OF STATES, AND INFINITESIMAL FERROMAGNETISM IN Ni, Pd, Pt

One of the quantities that is most important in determining the physical properties of a metal is the density of states at the Fermi level, $\eta(E_F)$. The electronic specific heat, the Pauli spin susceptibility, the transport properties, and the presence or absence of ferromagnetism, all depend on its value. This section will discuss the effects of the spin-orbit interaction and of hybridization of the conduction-band and d functions on $\eta(E_F)$, and will examine the relation of calculated values of $\eta(E_F)$ for the Ni, Pd, Pt sequence to specific-heat data, and to the criterion for infinitesimal ferromagnetism.

Figure 4 shows the density of states of paramagnetic Ni calculated for 16 384 points in the Brillouin zone. The solid curves refer to the unhybridized d and conduction bands and the dashed curve to the hybridized bands. The differences due to hybridization are quite significant; several large peaks appear to have shifted or disappeared completely. This behavior may readily be explained by reference to the diagram to the left, which shows the energy bands along the line from $\Lambda(222)$ to $U(282)$ and the approximate density-of-states curves for a narrow cylinder along this direction. The solid curves refer to the unhybridized bands. It will be noted, in particular, that there is a large peak at 0.53 Ry associated with a flat band at that energy. The hybridized bands include the dashed bands and the light solid bands (which do not hybridize with the conduction band). The large peak in the density of states at 0.53 Ry has been greatly reduced due to the hybridization between the flat band and the conduction band. It will also be noted that other peaks in the unhybridized density of states have changed in magnitude, and that hybridization has contributed new peaks at 0.30 and 0.33 Ry. Similar hybridization effects are also seen in the total density-of-states curve in the main diagram. It is to be expected on the basis of the large changes observed that hybridization between d and conduction bands may have a significant effect on the cohesive energy in the noble and transition metals. Mott[2] has suggested that this hybridization might be sufficient to account for the discrepancy between the observed cohesive energy of the noble metals and the contribution of the s electrons calculated by the Wigner-Seitz method.

Hybridization also affects the relative numbers of d and conduction electrons in the solid. In the hybridized bands of paramagnetic Ni, the Fermi level is raised 0.12 eV relative to the Fermi level of the unhybridized bands, and the approximate number of d electrons per atom is reduced from 8.95 to 8.82, while the number of conduction electrons per atom is increased from 1.05 to 1.18. It is to be noted that there are fewer than 9 d electrons per atom in solid Ni, rather than the 9.4 d electrons usually assumed. This results from the fact that the bottom of the conduction band in Hanus' APW

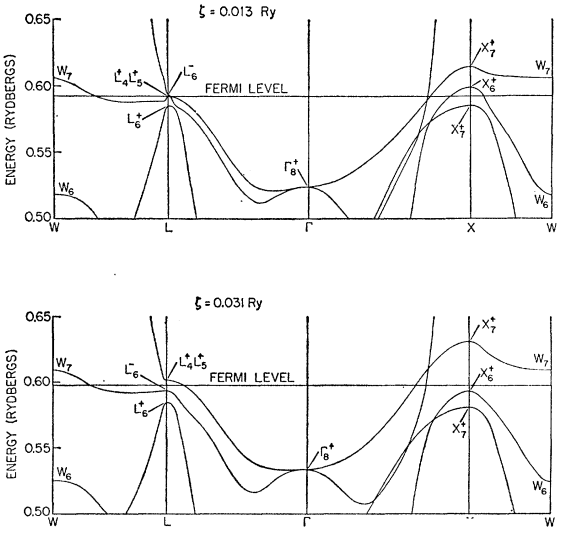

FIG. 5. Band structures corresponding to pseudopotential parameters for paramagnetic Ni and spin-orbit parameters of atomic Pd (top) and atomic Pt (bottom).

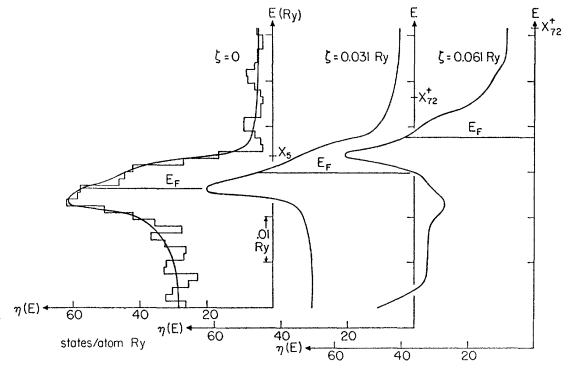

FIG. 6. Densities of states versus energy, in vicinity of Fermi level, showing how $\eta(E_F)$ decreases as the spin-orbit parameter is increased. X_{72}^+ (X_5 for $\zeta=0$) marks the top of the d band.

calculations[5] is situated well below all the pure d bands, with the result that the first conduction band is approximately half full (≈ 1 conduction electron per atom) at the Fermi level. There would be fewer conduction electrons and correspondingly more d electrons if the bottom of the conduction band were relatively higher. This is actually the case in the calculations of Yamashita *et al.*,[8] in which the Γ_1 level is situated 0.05 Ry below the Γ_{25}' level, compared to 0.45 Ry below in Hanus' calculations.[5] In Cu, the numbers of d and conduction electrons per atom are, respectively, 10 and 1 before hybridization, and 9.73 and 1.27 after hybridization. This reduction is due to the mixing of d wave functions into the upper unfilled conduction bands.

In order to study the effect of spin-orbit splitting on $\eta(E_F)$, it is necessary first to examine its influence on the band structure. The latter was calculated for $\zeta=0.013$ Ry (atomic Pd), 0.031 Ry (atomic Pt), and 0.061 Ry (twice atomic Pt value),[36] while the pseudopotential parameters of Sec. IIA were kept at values appropriate for paramagnetic Ni. This procedure permits the isolation of the effects of the spin-orbit interaction from those resulting from the widening and distortion of the bands in the descending Ni, Pd, Pt sequence.

Since the magnitude of ζ is determined by dU/dr near the nucleus, it is not unreasonable to assume atomic values. Studies on semiconductors,[46] as well as on Pb,[47] indicate, however, that ζ may be larger in the solid, and it is for this reason that a computation for $\zeta=2\zeta_{\text{at. Pt}}$ was done. A calculation for $\zeta=\zeta_{\text{at. Ni}}$ (0.0075 Ry) was not carried out because of the negligible effect of such a small splitting on $\eta(E_F)$.

The results for the case $\zeta=0$ are contained in Fig. 2; those corresponding to the atomic spin-orbit splitting of Pd and Pt are presented in Fig. 5. The most important effect of spin-orbit splitting is the removal of degeneracy, as at X_5 and L_{32}. Note that as ζ is increased, the uppermost band along L-Γ moves up, and its crossing with the next lower band moves toward L, ultimately occurring along W-L, where the bands hybridize. The spreading apart of the bands in the vicinity of the Fermi level as ζ is increased from zero can be expected to result in a decrease of the density of states in this region.

When $\zeta=0$, the upper d band is seen to be perfectly flat between W_1' and X_5 according to the present interpolation scheme. However, the introduction of spin-orbit coupling alters this behavior by raising one of the levels at X relative to that at W. This portion of the band, nevertheless, remains relatively flat and therefore a large resulting contribution to the density of states can be expected in a narrow energy range both with and without spin-orbit coupling.

The curves of Fig. 6 illustrate the change in the density of states in the vicinity of the Fermi level as ζ is increased. The curve for $\zeta=\zeta_{\text{at. Pd}}$ is very similar to that for $\zeta=0$, (Fig. 4) and is not shown. Note that as ζ increases, the peak at the Fermi level broadens out toward higher energies and becomes lower. In addition, the Fermi level shifts away from the highest part of the peak. These effects combine to reduce $\eta(E_F)$ with increasing ζ. This behavior, as deduced from the present calculation, is summarized in Fig. 7, which shows the dependence of $\eta(E_F)$ on ζ.

It should be pointed out that peaks such as those shown in Fig. 6 can result from relatively large regions in the Brillouin zone. The region giving rise to the peak at E_F in the density-of-states curve corresponding to $\zeta=0$ is shown in Fig. 8; note that this peak is less than 0.5-eV wide compared to a d-band width of about 4 eV. It is in large part the presence of the critical line between X_5 and W_1', for which $|\nabla_k E|=0$ when $\zeta=0$, that causes this narrow peak to arise from such a substantial region. Even with the introduction of spin-orbit coupling, $|\nabla_k E|$ remains approximately zero for this line.

Table II lists the computed values of $\eta(E_F)$, and experimental values of the electronic specific heat coefficient γ, expressed in terms of an $\eta(E_F)$ through the relation $\gamma=\frac{1}{3}\pi^2K^2\eta(E_F)$, where K is the Boltzmann constant. A comparison of these two sets of η is some-

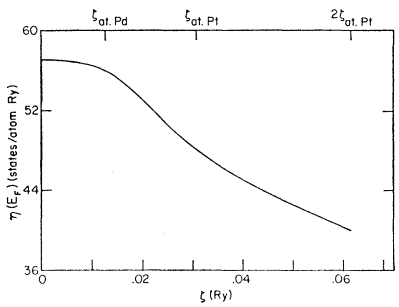

FIG. 7. Density of states at Fermi level versus spin-orbit parameter.

[46] R. Braunstein and E. O. Kane, J. Phys. Chem. Solids **23**, 1423 (1962).
[47] J. R. Anderson and A. V. Gold, Phys. Rev. **139**, A1459 (1965).

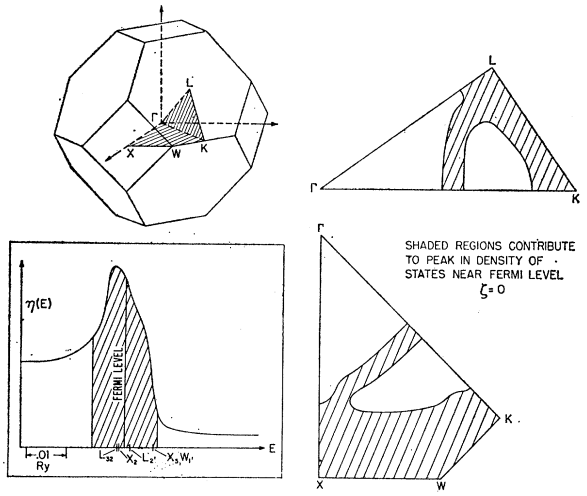

FIG. 8. Cross sections indicating regions in Brillouin zone responsible for large narrow peak in density of states near Fermi level for paramagnetic Ni. This peak is cross-hatched in plot of density of states versus energy (inset). Critical points required by symmetry in the energy range shown are marked.

what questionable because of the unknown contribution of dressing effects resulting from electron-phonon and electron-electron interactions. However, if one assumes, again on less than firm grounds, that the proportion of the experimental η contributed by dressing effects is roughly the same in each of the three cases, the qualitative features of the numbers in Table II may be examined. In Table II, an approximate value for $\gamma_{\text{para Ni}}$ was obtained by multiplying $\gamma_{\text{ferro Ni}}$ by the calculated ratio of $\eta(E_F)$ for paramagnetic and ferromagnetic Ni (see Sec. V). It is seen that an increase of ζ from zero to $\zeta_{\text{at. Pt}}$ reduces the calculated $\eta(E_F)$ by only 16%, whereas the $\eta(E_F)$ derived from γ_{Pt} is down by 50% from that for paramagnetic Ni. The relative discrepancy between the two reductions is even greater for Pd. It is clear too from the table that even if ζ were substantially larger in the solid, spin-orbit coupling alone would be insufficient to account for the observed reductions in $\eta(E_F)$.

Another question of interest is whether the calculated reductions of $\eta(E_F)$ in the Ni, Pd, Pt sequence can account for the absence of ferromagnetism in Pd and Pt, and its presence in Ni.[40] The criterion for infinitesimal ferromagnetism is easily derived by noting that

TABLE II. Comparison of calculated values of $\eta(E_F)$ with those derived from electronic-specific-heat data (Ref. 1).

ζ(Ry)	$\eta(E_F)$ (states/atom/Ry) calc.	expt.	Material
0 ($\approx$ at. Ni)	57	[80][a]	Paramagnetic Ni
0.013 (at. Pd)	56	54	Pd
0.031 (at. Pt)	48	39	Pt
0.061 (2×at. Pt)	40		

[a] This estimate is discussed in the text.

the paramagnetic system will be unstable to ferromagnetic ordering if its energy is lowered by reversing an infinitesimal number of spins δn. If the $J_{\text{eff}}^{s\text{-}d}$ term and the small conduction-electron contribution to the magnetization are neglected, then the change in paramagnetic band energy per particle is $(\delta n)^2/\eta_\sigma(E_F)$, where η_σ is the density of states for a single spin. The change in average correlation energy per particle is $-U_{\text{eff}}^{d\text{-}d}\sum_\mu(\delta n_\mu)^2$, which implies that infinitesimal ferromagnetism occurs when

$$U_{\text{eff}}^{d\text{-}d}\eta_\sigma(E_F)\sum_\mu(\delta n_\mu)^2/(\delta n)^2>1, \qquad (4.1)$$

where

$$\delta n=\sum_\mu \delta n_\mu.$$

The computations for paramagnetic Ni give $\sum_\mu(\delta n_\mu)^2/(\delta n)^2=0.25$, and from the results of Sec. V, $U_{\text{eff}}^{d\text{-}d}=0.195$ Ry. Using these values, Eq. (4.1) indicates that there will be infinitesimal ferromagnetism for an $\eta(E_F)$ in excess of 41 states/atom/Ry. The influence of spin-orbit coupling on $\eta(E_F)$ alone thus appears insufficient to explain the absence of ferromagnetism in Pd and Pt. An additional effect of importance is the probable reduction of $U_{\text{eff}}^{d\text{-}d}$ by spin-orbit coupling.[1] Another, and perhaps more significant, effect is the reduction of $\eta(E_F)$ by widening of the bands in the descending Ni, Pd, Pt sequence. The net effect, however, may be reduced somewhat by a corresponding increase of $U_{\text{eff}}^{d\text{-}d}$. That this widening occurs has been shown by the recent APW calculations for Pd by Freeman, Furdyna, and Dimmock[48] and for Pt by Mackintosh.[49]

V. FERROMAGNETIC Ni

Since all interpolation schemes rely heavily on experimental data in the adjustment of parameters, it is necessary, in the present applications to ferromagnetic Ni, to consider the relevant experimental data before discussing the calculated band structure and its physical consequences.

In Sec. IIC we have outlined the procedure for obtaining a ferromagnetic band structure, which involves fixing all parameters except $U_{\text{eff}}^{d\text{-}d}$ and $J_{\text{eff}}^{s\text{-}d}$ to a reliable first-principles band calculation for the paramagnetic state, and then determining $U_{\text{eff}}^{d\text{-}d}$ and $J_{\text{eff}}^{s\text{-}d}$ self-consistently using experimental data relating to the ferromagnetic state. As will be seen, $U_{\text{eff}}^{d\text{-}d}$ is determined largely by the requirement that the magneton number of ferromagnetic Ni should equal 0.55. The parameter $J_{\text{eff}}^{s\text{-}d}$, which has a very slight effect on the magneton number, is fixed by knowledge of the band structure near the point L, as determined from experiments relating to Fermi surfaces and the ferromagnetic Kerr effect (FKE). However, as we shall show, $J_{\text{eff}}^{s\text{-}d}$ is expected to be strongly $\mathbf{k}$ dependent and even to change

[48] A. J. Freeman, A. M. Furdyna, and J. O. Dimmock, J. Appl. Phys. 37, 1256 (1966).
[49] A. R. Mackintosh, Bull. Am. Phys. Soc. 11, 215 (1966).

sign somewhere inside the Brillouin zone. The experimental information therefore only determines J_{eff}^{s-d} in the outer parts of the zone. The pseudopotential method is ineffectual in describing the band structure in the vicinity of Γ_1 because of the lack of experimental data concerning band splittings in this region. More detailed information can only be obtained from unrestricted first-principles band calculations appropriate to the ferromagnetic state.

Although one might hope that only the parameters U_{eff}^{d-d} and J_{eff}^{s-d} need be fixed in passing from the paramagnetic to the ferromagnetic band structure, it will in fact be necessary to make slight changes in several of the parameters characterizing the paramagnetic state in order to optimize agreement with experiment. These changes correspond to fine adjustments and are no larger than the differences between the results of different first-principles calculations for the same metal.

A. Relevant Experimental Information

The saturation magnetization of ferromagnetic Ni is $0.606\mu_B$ per atom.[20] Since the spectroscopic splitting factor g is equal to 2.2, the spin and orbital moments must contribute, respectively, 0.551 and $0.055\mu_B$ per atom. The band structure of ferromagnetic Ni should then have an excess of 0.55 electrons of one spin, or approximately 5.275 majority-spin electrons and 4.725 minority-spin electrons.

The spatial distribution of the magnetization has been determined by Mook and Shull[23] by a Fourier inversion of the magnetic form factor obtained from their neutron-diffraction experiments. The net spin density along the [100] direction is shown in Fig. 9. The large hump near the nucleus is due primarily to d electrons. The net-spin-density curve crosses zero at approximately the shell radius of atomic Ni^{++},[50] and subsequently the spin density is negative and almost constant. This behavior is most easily reconciled with an apparent conduction-band spin density polarized oppositely to that of the d electrons. Mook and Shull[23] have analyzed their experimental form factor on this basis, assuming that the conduction electrons may be represented by plane waves whose polarization is constant throughout the unit cell and opposite to that of the d electrons. Good agreement with experiment was obtained by using an atomic form factor to represent the d contribution and by assuming that the net reverse polarization of the conduction electrons amounts to 19% of the magneton number. They have also obtained the correct asymmetry of the form factor at large reflections by assuming the distribution of the magnetic electrons to correspond to 81% in T_{2g} orbitals and 19% in E_g orbitals.

[50] L. Pauling, *The Nature of the Chemical Bond* (Cornell University Press, Ithaca, New York, 1960), p. 518.

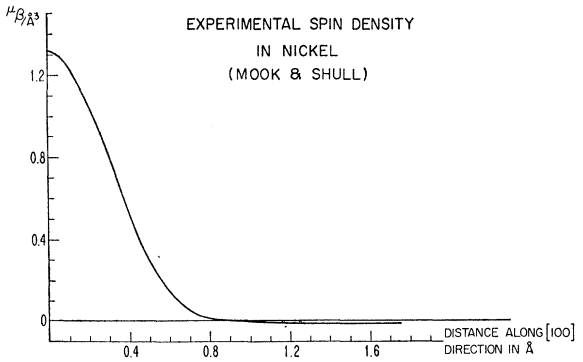

FIG. 9. The experimental spin density in Ni along the [100] direction in Bohr magnetons per Å^3 as determined by Mook and Shull (Ref. 23).

There are two essential difficulties with this explanation, however. First, the presence of a reverse polarization of the conduction electrons is inconsistent with the s-d exchange coupling discussed in Sec. IIC. Second, as we shall discuss below, it is far easier to explain the results of Fermi surface and magneto-optical experiments on the basis of a band structure, consistent with a positive conduction-electron polarization in the outer parts of the Brillouin zone (or the inner regions of the unit cell), in which the minority-spin conduction bands at the Fermi level are higher in energy than those of the majority spins.

A possible answer to these difficulties may be connected with the importance of the fact that the wave functions corresponding to spin ↑ and ↓ may differ appreciably. In an unrestricted Hartree-Fock calculation for atomic Fe in the $3d^64s^2$ configuration, Freeman and Watson[44] found that the $4s$ spin density, although integrating to zero, is essentially positive in the region near the nucleus where the dominant d-electron polarization occurs, and is negative for larger value of r. A similar effect may very well occur for the conduction electrons in the ferromagnetic solid, leading to the kind of spin distribution shown in Fig. 9, in which the conduction-electron polarization is positive near the nucleus and negative in the outer parts of the unit cell, the net polarization being small but positive. Therefore, in $\mathbf{k}$ space the minority-spin conduction bands would be expected to be higher in energy than the majority-spin bands in the outer parts of the Brillouin zone, but lower near $\mathbf{k}=0$. As already pointed out, there is at present no experimental information pertinent to the behavior near $\mathbf{k}=0$. Such effects can only be incorporated into the present pseudopotential method by regarding J_{eff}^{s-d} to be $\mathbf{k}$ dependent instead of constant.

The interpretation of the neutron-diffraction data which emerges from the present work, and which will be discussed in Sec. VI, differs from that of Mook and Shull.[23] We shall show that there is a small positive net conduction-electron polarization predicted by the present ferromagnetic band structure. The d-electron

contribution, obtained from unrestricted atomic wave functions, will also permit an estimate of the contribution of the paired electrons. According to the present picture, the observed asymmetry of the magnetic form factor at large reflections requires that 86% and 14% of the uncompensated majority spin electrons be, respectively, in T_{2g} and E_g orbitals, rather than 81% and 19% as in the analysis of Ref. 23.

Recent Fermi-surface experiments[9] have also shed some light on the band structure of ferromagnetic Ni by imposing several conditions concerning the topology of the Fermi surface. One surface must be multiply connected as in Cu, with necks protruding in the [111] directions. The neck radius measured by de Haas-van Alphen experiments is 0.09 Å^{-1}. The other surfaces must be such as to yield a high-field Hall coefficient of exactly unity. In terms of the type of parameter-fitting characterizing the present work, the actual information obtained from these experiments is rather minimal. Any reasonable band structure agrees with the high-field Hall-coefficient measurements. The existence of necks indicates that the L_2' level for the majority spins is situated just below the Fermi level. Slight shifts in the overlap of the d and conduction bands, corresponding to minute changes in two of the parameters (E_0 and β), seriously affect the size and even the existence of necks at L. However, much larger changes would be necessary if we had started with a paramagnetic band structure having a smaller s-d separation, such as that of Yamashita *et al.*[8] When more complete Fermi-surface experiments are available, a more satisfactory fit may be possible using the approach of Gold[51] and Anderson.[47]

The important information about the electronic structure of ferromagnetic metals to be gained from a study of the FKE has been stressed by Ehrenreich, Philipp, and Olechna,[30] Phillips,[32] and Cooper and Ehrenreich.[52,53] The experimentally observed structure in the FKE in Ni can be attributed to optical transitions involving d and conduction bands for minority spins near L. This interpretation fixes the approximate locations of the L_3 and L_2' levels for minority spins at 0.24 eV above the Fermi level.[52–54] These levels can be placed correctly by a proper choice of J_{eff}^{s-d} and by a slight adjustment in one of the pseudopotential parameters. An alternative model of the band structure due to Phillips[32] has been shown[52,53] to be inconsistent with the FKE without modification.

B. Band Structure and Its Implications

In our self-consistent calculations of the ferromagnetic band structure of Ni, we have used the values $U_{\text{eff}}^{d-d}=2.65$ eV and $J_{\text{eff}}^{s-d}=0.6$ eV. A detailed calculation indicates that the magneton number ν corresponding to these values is 0.58, of which approximately 97.5% is due to d-electron polarization and the other 2.5% to conduction-electron polarization. Since ν is a little larger than the experimental value of 0.55, U_{eff}^{d-d} should be slightly smaller, close to 2.5 eV.

As mentioned earlier, it was necessary to alter several of the paramagnetic parameters determined in Sec. IIA very slightly in order to optimize agreement between the ferromagnetic band structure and experiment. The positioning of the L_3 level for minority spins approximately 0.24 eV above the Fermi level, as required by the interpretation of the FKE,[52] necessitates a slight raising of the level from its position in Hanus' paramagnetic bands. The small energy increase of less than 0.2 eV is easily produced in the context of the present interpolation scheme by an increase in the magnitude of A_3 or A_6 or both parameters. For simplicity we have adjusted only A_3, increasing the value obtained from Hanus' bands by 30%. This is not unreasonable, since some of the parameters determined from different first-principles calculations, such as those of Burdick[4] and Segall[3] for Cu, differ by more than this. This raising of the L_3 level does not affect the position of the Fermi level appreciably, since the contribution of the surrounding region to the density of states is small.[55] Accordingly, the FKE plays an unimportant role in the determination of the gross features of the band structure. It nevertheless is sensitively related to the details of the Fermi surface.

As mentioned in Sec. VA and discussed more fully in Sec. VI, the asymmetry of the magnetic form factor requires 14% of the uncompensated majority-spin electrons to be in E_g orbitals. The unadjusted pseudopotential parameters determined from Hanus's[5] bands result in too few E_g electrons near the Fermi surface. This situation may be remedied in several ways. In the absence of more experimental information concerning the region near the Fermi surface, it is not clear which of the parameters should be altered. Accordingly, we have adopted the simplest alternative of increasing the value of the crystal-field parameter Δ by 0.3 eV. This corresponds to increasing the $\Gamma_{12}-\Gamma_{25}'$ energy difference by 0.3 eV, a change which is of the same order as the

[51] A. V. Gold, Phil. Trans. Roy. Soc. (London) **A251**, 85 (1958).

[52] B. R. Cooper and H. Ehrenreich, Solid State Commun. **2**, 171 (1964); B. R. Cooper, Phys. Rev. **139**, A1504 (1965); B. R. Cooper, H. Ehrenreich, and L. Hodges, in *Proceedings of the International Conference on Magnetism, Nottingham, England, 1964* (Institute of Physics and the Physical Society, London, 1965), p. 110.

[53] H. Ehrenreich, in *Proceedings of the International Colloquium on Optical Properties and Electronic Structure of Metals and Alloys, Paris, 1965* (North-Holland Publishing Company, Amsterdam, 1966).

[54] A similar model was proposed by G. S. Krinchik [in *Proceedings of the International Colloquium on Optical Properties and Electronic Structure of Metals and Alloys, Paris, 1965* (North-Holland Publishing Company, Amsterdam, 1966)], but contradicts that discussed in another publication: G. S. Krinchik and E. S. Banin, Zh. Eksperim. i Teor. Fiz. **49**, 470 (1965) [English transl.: Soviet Phys.—JETP **22**, 331 (1966)].

[55] Phillips' statement (see Ref. 32) to the effect that such an adjustment was inconsistent with the correct value of the magneton number was apparently based on the supposition that the entire band structure would be shifted by 0.2 eV. This is clearly not required.

corresponding difference in Segall's[3] (0.98 eV) and Mattheiss's[6] (0.54 eV) calculations for Cu.

In addition, the value of the parameter β has been increased by 0.3 eV, corresponding to a raising of the Γ_1 level at the bottom of the conduction band. This change again is very small compared to differences among various band calculations. Snow, Waber, and Switendick[56] have described the origin of these differences in the relative positions of the conduction and d bands in terms of the atomic-electronic configuration assumed in constructing the crystal potential. Thus Hanus[5] may not have employed the optimum atomic configuration in his calculations. Wakoh and Yamashita[8] have also discussed this problem and pointed out that while Hanus obtained a reasonable separation, his potential violated the condition of charge neutrality in the unit cell. Another reason for the adjustments may be connected with the necessity of using a more realistic version of the Coulomb interaction than that discussed in Sec. IIC. However, the fact that only relatively small changes in the values of three parameters (A_3, Δ, and β) are required in order to adjust Hanus' calculations implies that they represent a reasonably realistic version of the expected paramagnetic band structure.

The self-consistently calculated electronic energy bands of ferromagnetic Ni are plotted along several symmetry lines in Fig. 10. A cursory inspection of Fig. 10 indicates the d-band splittings to be essentially rigid, as has been previously supposed. In fact, however, the present effective Coulomb Hamiltonian does lead to some $\mathbf{k}$ dependence in the splitting which may be increased even further when more realistic versions of this interaction are considered in band calculations. The origin of this $\mathbf{k}$ dependence was discussed in Sec. IIC and will now be recapitulated.

The Bloch eigenfunctions of the full Hamiltonian are linear combinations of three types of basis functions: OPW's, and LCAO's having T_{2g} and E_g symmetry. The $\mathbf{k}$ dependence of the exchange splitting then arises from the fact that each type of basis function is characterized by its own splitting when the ferromagnetic interaction [see Eq. (2.23)] is taken into account. The exchange splittings of pure T_{2g} and E_g levels are, respectively, 0.42 and 0.10 eV in the present self-consistent calculations. The average splitting of the d bands is 0.29 eV, but is a little larger (0.37 eV) in the neighborhood of the Fermi surface because of the preponderance of T_{2g} orbitals. The exchange splitting of the conduction levels is 0.36 eV near the zone faces and is unknown in the interior of the Brillouin zone.

It may be of interest to compare these exchange splittings with other recent estimates. It is now clear that the value given by Ehrenreich, Philipp, and Olechna[30] was too large, since it resulted from a simple

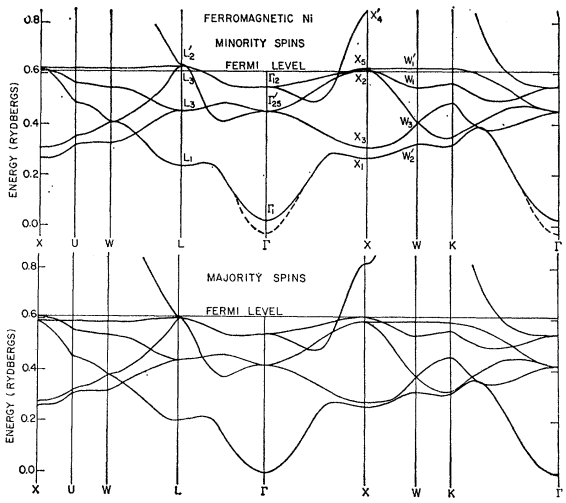

FIG. 10. Calculated ferromagnetic band structure of Ni along selected symmetry lines. The dashed lines suggest the possible lowering of the minority-spin conduction bands near the center of the zone relative to those of the majority spins due to a reversal in sign of the effective s-d exchange energy (see text).

superposition of Cu and Ni bands for majority and minority spins, respectively. However, as emphasized in their paper, the Fermi surfaces obtained were likely to be consistent with experiment provided the majority d bands were filled. It will be seen that the Fermi surfaces of the present work are topologically equivalent to them. The exchange splitting of the d bands given by Phillips[32] (0.6–0.8 eV) is also significantly larger than that of the present calculations, presumably due to the fact that this result is based on relatively rough numerical estimates as well as on an interpretation of the FKE with which we disagree.[57] Herring has empirically estimated the exchange splitting to be 0.25 eV in two different ways, and stated that a value in excess of about 0.35–0.40 eV could be accounted for only on the basis of a large electron-phonon interaction. In making these comparisons, it should be emphasized that the present $U_{\text{eff}}{}^{d\text{-}d}$, proportional to the exchange splitting, differs in definition from that used by Herring[58]: It is necessary to multiply the value that he gives by three. In terms of our definition, his estimate of $U_{\text{eff}}{}^{d\text{-}d}=1.25$ eV is smaller than ours ($U_{\text{eff}}{}^{d\text{-}d}\approx 2.5$ eV) by a factor of two. However, a strong electron-phonon interaction would influence the magnitude of U_{eff} in the same manner as the exchange splitting. Some information concerning this interaction can frequently be obtained

[56] E. C. Snow, J. T. Waber, and A. C. Switendick, J. Appl. Phys. **37**, 1342 (1966).

[57] The reasons for doubting certain features of Phillips' interpretation of the FKE were discussed in Refs. 52 and 53.

[58] This may be seen most directly by a comparison of the criterion for ferromagnetism of Eq. (4.1) with that of Herring, who has assumed that there are only holes in the d band of Ni which exist in the states near X_5 composed of linear combinations of the three T_{2g} orbitals. Thus, $[\sum_\mu (\delta n_\mu)^2/(\delta n)^2]=\frac{1}{3}$. Herring's criterion is that $U_{\text{eff}}\eta(E_F)>1$, where $\eta(E_F)$ is the density of states at the Fermi level for a single spin. Accordingly, the equation $U_{\text{eff}}=\frac{1}{3}U_{\text{eff}}{}^{d\text{-}d}$ relates Herring's U_{eff} to the quantity $U_{\text{eff}}{}^{d\text{-}d}$ of the present work.

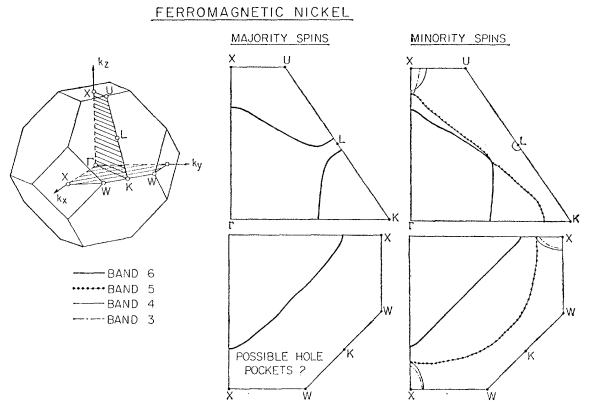

FIG. 11. Selected cross sections of the majority- and minority-spin Fermi surfaces for ferromagnetic Ni. The five d bands and lowest conduction band have been labeled 1, ···, 6 in order of increasing energy. The existence of possible small majority-spin hole pockets is discussed in the text.

from an experimental value for the electronic specific heat.[59] We shall later make an estimate of this quantity for Ni which shows that the results of the present calculation account for $\frac{2}{3}$ of the experimentally observed value. If we assume the difference to be accounted for by the electron-phonon interaction (a fact not yet established theoretically), then the d-band width assumed by Herring should be increased by 50% and his new estimate of U_{eff} would correspond to $U_{\text{eff}}^{d\text{-}d}=1.8$ eV, in better agreement with the present calculation. Our results also agree well with the value of 0.4 eV at the top of the d band obtained by Hubbard,[60] and with Wohlfarth's[61] summary value of (0.35 ± 0.05) eV.

It should be emphasized that the value of the parameter $J_{\text{eff}}^{s\text{-}d}$ cannot be fixed with precision because the exact positions of the majority and minority spin L_2' levels relative to the Fermi level are not established by the FKE and Fermi experiments discussed in Sec. VA. $J_{\text{eff}}^{s\text{-}d}$ is also presumably $\mathbf{k}$-dependent, as discussed above. Indeed, the reverse spin polarization in the outer parts of the unit cell obtained from neutron-diffraction experiments suggests that an unrestricted band calculation would show the bottom of the conduction band to be lower for minority than for majority spins. This possibility has been suggested qualitatively by the use of dashed lines to denote the band structure near $\mathbf{k}=0$ in Fig. 10.

Table III shows the distribution of majority and minority spin electrons among d and conduction levels and their respective contributions to the magneton number. We shall make use of these values in Sec. VI to compute the neutron magnetic form factor. It should be noted that there are only about 4.7 majority-spin d electrons, not the 5.0 usually assumed. This reduction results from the mixing of d wave functions into the unfilled majority-spin conduction bands. The reason for the relatively large number of conduction-band electrons has already been discussed in Sec. IV.

Figure 11 shows selected cross sections of the Fermi surfaces obtained from the ferromagnetic band structure of Fig. 10. The majority spins have a single electron surface with necks protruding along the [111] directions. The minimum neck radius of ≈ 0.07 Å^{-1} falls within the range of experimental values reported by Joseph and Thorsen.[9] The minority spins have two electron surfaces, plus hole pockets in two lower bands. There are majority-spin energy levels at X and W that are very near the Fermi level, as may be seen in Fig. 10. The exact location of these levels with respect to the Fermi level cannot be precisely ascertained, since only very small changes in the pseudopotential parameters are necessary to place these levels slightly above or below the Fermi energy. It is, therefore, uncertain whether or not there are hole pockets in the majority-spin bands. For the same reason, the hole pockets in the minority-spin bands may be displaced somewhat from the positions shown in Fig. 11. Until a more detailed experimental mapping of the Fermi surface is available, it is not possible to fix the exact shapes of the various surfaces.

The calculated density-of-states curves for ferromagnetic Ni are shown in Fig. 12. The contributions for each spin are shifted by about 0.3 eV and resemble, but are not identical with, those corresponding to paramagnetic Ni shown in Fig. 4. The differences in shapes arise from the $\mathbf{k}$ dependence of the exchange splitting. The large peak near the top of the d-band complex is somewhat higher than that for the paramagnetic state because of the adjustment made in the value of Δ. The approximate densities of states per atom at the Fermi level are 22.6 states/Ry for the minority-spin electrons and 4.5 states/Ry for the majority-spin electrons, resulting in a total of 27.1 states/Ry. This value corresponds to an electronic specific heat of 1.12×10^{-3} cal/mole deg^2, which is about $\frac{2}{3}$ of the experimental value[22] of 1.68×10^{-3} cal/mole deg^2. Because the electron-phonon and electron-electron interactions are known to influence the electronic specific heat significantly,[59] this sort of discrepancy is not surprising. The implication of the electron-phonon

TABLE III. Distribution of majority- and minority-spin electrons in ferromagnetic Ni.

	Majority	Minority	Difference
$n(T_{2g})$	2.82	2.34	0.49
$n(E_g)$	1.88	1.80	0.08
total d	4.71	4.14	0.57
$n(s)$	0.58	0.57	0.01
total	5.29	4.71	0.58

[59] A. M. Clogston, Phys. Rev. **136**, A8 (1964); N. W. Ashcroft and J. W. Wilkins, Phys. Letters **14**, 285 (1965); W. A. Harrison (Ref. 19).

[60] J. Hubbard, Proc. Phys. Soc. (London) **84**, 455 (1964).

[61] E. P. Wohlfarth, in *Proceedings of the International Conference on Magnetism, Nottingham, England, 1964* (Institute of Physics and the Physical Society, London, 1965), p. 51.

interaction on the magnitude of U_{eff} has already been discussed.

The present calculations may be used to predict the high-field band susceptibility χ_d at $T=0°$K. In the present theory, the usual formula for the susceptibility per atom in the collective electron theory of ferromagnetism[62] is replaced by

$$\frac{\mu_B^2}{\chi_d}=\frac{1}{4}\left[\frac{1}{\eta_\uparrow(E_F)}+\frac{1}{\eta_\downarrow(E_F)}\right]-\tfrac{1}{2}U_{\text{eff}}{}^{d\text{-}d}\sum_\mu \tilde{n}_{\mu\uparrow}\tilde{n}_{\mu\downarrow}$$
$$-\tfrac{1}{2}J_{\text{eff}}{}^{s\text{-}d}(\tilde{n}_{s\uparrow}-\tilde{n}_{s\uparrow}{}^2+\tilde{n}_{s\downarrow}-\tilde{n}_{s\downarrow}{}^2),$$

where $\eta_\uparrow(E_F)$ and $\eta_\downarrow(E_F)$ are the densities of states per atom of $\uparrow$ and $\downarrow$ spins, respectively. In order to define the quantities $\tilde{n}_{\mu\sigma}$ and $\tilde{n}_{s\sigma}$, we note that in applying a large magnetic field to a ferromagnet, the populations of the orbitals $\mu\sigma$ will change by amounts $\delta n_{\mu\sigma}$. In terms of this change, $\tilde{n}_{\mu\sigma}=|\delta n_{\mu\sigma}/\delta n|$, where $\delta n=\delta n_{s\uparrow}+\sum_\mu \delta n_{\mu\uparrow}$ $=-\delta n_{s\downarrow}-\sum_\mu \delta n_{\mu\downarrow}$. Similarly, $\tilde{n}_{s\sigma}=|\delta n_{s\sigma}/\delta n|$. On the basis of the present calculations, a value for χ_d of 0.8×10^{-5} emu/cm^3 is predicted for Ni. This is considerably smaller than the value of 4×10^{-5} emu/cm^3 estimated by Herring *et al.*,[25] but is not negligible as Freeman *et al.* have suggested.[24] The smallness of χ_d is due to the low density of states of majority-spin electrons. It should be noted, as pointed out earlier in connection with the description of the Fermi surfaces, that there may be hole pockets in the majority-spin bands. The presence of these holes would increase the value $\eta(E_F)$ for majority-spin electrons, although this increase would not be very large if the hole pockets were small. Such an effect would increase the claculated value of χ_d.

VI. MAGNETIC FORM FACTOR OF Ni

This section is devoted to a discussion of the neutron magnetic form factor in band-theoretic terms and its calculation for Ni using the ferromagnetic band structure of Sec. V. A formal treatment of this problem along band-theoretic lines for a simplified model has been previously given by Izuyama, Kim, and Kubo.[63] However, to our knowledge, no attempt at numerical application involving a realistic band structure has been made previously.

The neutron magnetic form factor $f(\boldsymbol{\kappa})$ is defined as the ratio of the magnetic scattering amplitude for a given scattering vector $\boldsymbol{\kappa}$ to that for $\boldsymbol{\kappa}=0$. It may be written as a sum of three contributions:

$$f(\boldsymbol{\kappa})=(2/g)f_{\text{spin}}(\boldsymbol{\kappa})+[(g-2)/g]f_{\text{orb}}(\boldsymbol{\kappa})+f_{\text{core}}(\boldsymbol{\kappa}), \quad (6.1)$$

where g is the spectroscopic splitting factor. Further, f_{spin} is the form factor for the spin magnetic moment of electrons outside the core, normalized so that $f_{\text{spin}}(0)=1$. The core itself has a net spin of zero [which is seen to imply that $f_{\text{core}}(0)=0$], but the slight difference due to exchange effects in the radial distributions for up and down spins causes some scattering by the core, which leads to a small, but nonvanishing f_{core}. This term has been discussed by Watson and Freeman.[42] The orbital magnetic moment gives rise to a form factor f_{orb} for which $f_{\text{orb}}(0)=1$. This quantity has been discussed by Blume.[64]

The term $f_{\text{spin}}(\boldsymbol{\kappa})$, which makes the dominant contribution to the total form factor, is given by $f_\uparrow(\boldsymbol{\kappa})-f_\downarrow(\boldsymbol{\kappa})$, where

$$f_\sigma(\boldsymbol{\kappa})=(N\nu)^{-1}\int e^{i\boldsymbol{\kappa}\cdot\mathbf{r}}\rho_\sigma(\mathbf{r})d^3r, \quad (6.2)$$

and ν is the magneton number. If $\rho_\sigma(\mathbf{r})$ is the periodic electron density of spin σ, then $f_\sigma(\boldsymbol{\kappa})$ vanishes unless $\boldsymbol{\kappa}$ is a reciprocal lattice vector.

The spin density can be found from

$$\rho_\sigma(\mathbf{r})=\sum_{n\mathbf{k}\text{ occ}}|B_{kn\sigma}(\mathbf{r})|^2, \quad (6.3)$$

where $B_{kn\sigma}(\mathbf{r})$ are the Bloch functions which are given approximately by Eq. (2.3). The adequacy of the functions (2.3) for calculations of the charge density has already been discussed in Sec. III. However, in order to make the following treatment formally correct, let us begin with the rigorously correct Bloch functions, whose conduction-band portion contains explicit orthogonalization both to d and core functions, and postpone approximations until later. To denote this more extended orthogonalization, we replace the symbol "d" in the OPW $\langle\mathbf{r}|\mathbf{k}+\mathbf{K};\sigma,d\rangle$ by "core+d."

Substituting Eqs. (2.3) and (6.3) into (6.2), we obtain[65]

$$f_\sigma(\boldsymbol{\kappa})=(N\nu)^{-1}\sum_{n\mathbf{k}\text{ occ.}}\int d^3r\, e^{i\boldsymbol{\kappa}\cdot\mathbf{r}}$$
$$\times\{\sum_{\mathbf{K}\mathbf{K}'}a_{n\mathbf{K}\sigma}{}^*(\mathbf{k})a_{n\mathbf{K}'\sigma}(\mathbf{k})$$
$$\times\langle\mathbf{k}+\mathbf{K},\sigma;\text{core}+d|\mathbf{r}\rangle\langle\mathbf{r}|\mathbf{k}+\mathbf{K}',\sigma;\text{core}+d\rangle$$
$$+2\,\text{Re}\sum_{\mathbf{K}\mu}a_{n\mathbf{K}\sigma}{}^*(\mathbf{k})a_{n\mu\sigma}(\mathbf{k})$$
$$\times\langle\mathbf{k}+\mathbf{K},\sigma;\text{core}+d|\mathbf{r}\rangle\langle\mathbf{r}|\mathbf{k}\mu\sigma\rangle$$
$$+\sum_{\mu\mu'}a_{n\mu\sigma}{}^*(\mathbf{k})a_{n\mu'\sigma}(\mathbf{k})\langle\mathbf{k}\mu\sigma|\mathbf{r}\rangle\langle\mathbf{r}|\mathbf{k}\mu'\sigma\rangle\}, \quad (6.4)$$

which can be written schematically as

$$f_\sigma=f_\sigma{}^{\text{OPW-OPW}}+f_\sigma{}^{\text{OPW-}d}+f_\sigma{}^{d\text{-}d}. \quad (6.5)$$

[62] E. P. Wohlfarth, Phys. Letters **3**, 17 (1962).

[63] T. Izuyama, D. J. Kim, and R. Kubo, J. Phys. Soc. Japan **18**, 1025 (1963).

[64] M. Blume, Phys. Rev. **124**, 96 (1961).

[65] It should be noted that in Eq. (6.4) and later equations, the sums on $\mathbf{k}$ extend over all occupied states in the Brillouin zone. Thus the sums over $\mathbf{K}$ and $\mathbf{K}'$ must be taken to range over the 15 different reciprocal lattice vectors appropriate to the OPW's in all parts of the zone, not just the four values included in Sec. IIA for the 1/48 of the zone in which the calculations were carried out.

The first term of Eq. (6.5) becomes, upon use of the explicit expression for the OPW's, Eq. (2.5),

$$f_\sigma^{\text{OPW-OPW}}(\boldsymbol{\kappa})=(N\nu)^{-1}\sum_{n\mathbf{k}\text{ occ}}\sum_{\mathbf{K}\mathbf{K}'}a_{n\mathbf{K}\sigma}{}^*(\mathbf{k})a_{n\mathbf{K}'\sigma}(\mathbf{k})(\mathfrak{N}_{\mathbf{k}\mathbf{K}}\mathfrak{N}_{\mathbf{k}\mathbf{K}'})^{-1/2}$$
$$\times\{\langle\mathbf{k}+\mathbf{K},\sigma|\mathbf{k}+\mathbf{K}'+\boldsymbol{\kappa},\sigma\rangle-\sum_\tau[\langle\mathbf{k}+\mathbf{K},\sigma|\mathbf{k}\tau\sigma\rangle\langle\mathbf{k}\tau\sigma|\mathbf{k}+\mathbf{K}'+\boldsymbol{\kappa},\sigma\rangle+\langle\mathbf{k}+\mathbf{K}-\boldsymbol{\kappa},\sigma|\mathbf{k}\tau\sigma\rangle\langle\mathbf{k}\tau\sigma|\mathbf{k}+\mathbf{K}',\sigma\rangle]$$
$$+\sum_{\tau\tau'}\langle\mathbf{k}+\mathbf{K},\sigma|\mathbf{k}\tau\sigma\rangle\langle\mathbf{k}\tau\sigma|e^{i\boldsymbol{\kappa}\cdot\mathbf{r}}|\mathbf{k}\tau'\sigma\rangle\langle\mathbf{k}\tau'\sigma|\mathbf{k}+\mathbf{K}',\sigma\rangle\}\,, \quad (6.6)$$

where the index τ refers to core and d functions and $\mathfrak{N}_{\mathbf{k}\mathbf{K}}$ is defined in Eq. (2.6). This term may be estimated relatively roughly since the total contribution of $f_\sigma^{\text{OPW-OPW}}$ to f_{spin} is not very great, the coefficients $a_{n\mathbf{K}\sigma}{}^*a_{n\mathbf{K}'\sigma}$ being small for the energy region of interest. In addition, if the matrix elements in this equation were the same for both spins, the coefficient of these terms in the expression for f_{spin} would be $a_{n\mathbf{K}\uparrow}{}^*a_{n\mathbf{K}'\uparrow}-a_{n\mathbf{K}\downarrow}{}^*a_{n\mathbf{K}'\downarrow}$, which is particularly small, since there is little polarization of the conduction band. We note that all but the first term in Eq. (6.6) may be neglected since the remaining ones involve two factors of the orthogonalization form $\langle\mathbf{k}+\mathbf{K}|\mathbf{k}\tau\rangle$ and thus are expected to contribute little.

As may be seen from Eq. (2.6), the normalization factor $(\mathfrak{N}_{\mathbf{k}\mathbf{K}}\mathfrak{N}_{\mathbf{k}\mathbf{K}'})^{-1/2}$ is relatively close to unity, even when core terms are included. It will be assumed to have this value here. The pure conduction-band part of f_σ is then approximately given by the plane-wave (PW) components:

$$f_\sigma^{\text{OPW-OPW}}(\boldsymbol{\kappa})\approx f_\sigma^{\text{PW-PW}}(\boldsymbol{\kappa})$$
$$=(N\nu)^{-1}\sum_{n\mathbf{k}\text{ occ}}\sum_{\mathbf{K}\mathbf{K}'}a_{n\mathbf{K}\sigma}{}^*(\mathbf{k})a_{n\mathbf{K}'\sigma}(\mathbf{k})\delta_{\boldsymbol{\kappa},\mathbf{K}-\mathbf{K}'}\,. \quad (6.7)$$

The second term in Eq. (6.5), $f_\sigma^{\text{OPW-}d}$, can be analyzed in a manner similar to that used for $f_\sigma^{\text{OPW-OPW}}$. All of its component terms are found to include one factor of the small coefficient $a_{n\mathbf{K}\sigma}$ and one factor of the relatively small integral $\langle\mathbf{k}+\mathbf{K}|\mathbf{k}\tau\rangle$, as opposed to two of such factors in each of the omitted terms of $f_\sigma^{\text{OPW-OPW}}$. While the cross term $f_\sigma^{\text{OPW-}d}$, therefore, should not be large, the justification for neglecting it is not nearly so clear as that for the omitted terms of $f_\sigma^{\text{OPW-OPW}}$. It might be mentioned, however, that the portion of this term which is expected to be dominant is zero at $\boldsymbol{\kappa}=0$, and drops off rapidly for large $\boldsymbol{\kappa}$, while a very rough estimate indicates that it has its maximum effect in the vicinity of the first nonzero value of $\boldsymbol{\kappa}$.

In light of the previous approximations, Eq. (6.5) becomes

$$f_\sigma\approx f_\sigma^{\text{PW-PW}}+f_\sigma^{d\text{-}d}\,. \quad (6.8)$$

In the preceding treatment, the PW terms have been treated as though they were really part of a complete OPW conduction-band wave function. As emphasized in Sec. III, however, the $a_{n\mathbf{K}\sigma}$ can be regarded as containing at least some of the features resulting from the d and core function orthogonalization because the pseudopotential parameters were determined to make the energy eigenvalues conform to the actual band structure. Thus some part of the contribution from terms that were apparently entirely neglected above is undoubtedly present in our numerical results, and the approximations, accordingly, especially concerning $f_\sigma^{\text{OPW-}d}$, may not be as severe as they seem. In this connection, however, one should bear in mind again that the predominant contribution to the magnetic form factor arises from $f_\sigma^{d\text{-}d}$ which can be calculated without these difficulties. It should also be mentioned that for very large values of $\boldsymbol{\kappa}$, neglect of the core orthogonalization will not be valid. The contribution of these terms, though probably not large, drops off more slowly than that of the other terms as $\boldsymbol{\kappa}$ increases, and hence will be relatively more important.

In order to simplify $f_\sigma^{d\text{-}d}$ further, we note that symmetry arguments show that $\sum_{n\mathbf{k}\text{ occ}}a_{n\mu\sigma}{}^*(\mathbf{k})a_{n\mu'\sigma}(\mathbf{k})=0$ for $\mu\neq\mu'$. Hence the second term in Eq. (6.8) can be written

$$f_\sigma^{d\text{-}d}(\boldsymbol{\kappa})=(N\nu)^{-1}\sum_{n\mathbf{k}\text{ occ}}\sum_\mu|a_{n\mu\sigma}(\mathbf{k})|^2$$
$$\times\langle\mathbf{k}\mu\sigma|e^{i\boldsymbol{\kappa}\cdot\mathbf{r}}|\mathbf{k}\mu\sigma\rangle\,. \quad (6.9)$$

With the notation $\langle j_n\rangle_\kappa{}^{\mu\sigma}=\int_0^\infty[rf^{\mu\sigma}(r)]^2j_n(\kappa r)d^3r$, this term can be put in the form[66]:

$$f_\sigma^{d\text{-}d}(\boldsymbol{\kappa})=(N\nu)^{-1}\{[\langle j_0\rangle_\kappa{}^{T_{2g}\sigma}-A(hkl)\langle j_4\rangle_\kappa{}^{T_{2g}\sigma}]$$
$$\times\sum_{n\mathbf{k}\text{ occ}}\sum_{\mu=1}^{3}|a_{n\mu\sigma}(\mathbf{k})|^2$$
$$+[\langle j_0\rangle_\kappa{}^{E_g\sigma}+\tfrac{3}{2}A(hkl)\langle j_4\rangle_\kappa{}^{E_g\sigma}]$$
$$\times\sum_{n\mathbf{k}\text{ occ}}\sum_{\mu=4}^{5}|a_{n\mu\sigma}(\mathbf{k})|^2\}\,, \quad (6.10)$$

where

$$A(hkl)=(h^2+k^2+l^2)^{-2}[h^4+k^4+l^4-3(h^2k^2+h^2l^2+k^2l^2)].$$

Here h, k, l are the Miller indices of the scattering plane. The terms involving $\langle j_0\rangle_\kappa$ comprise the spherical part of the form factor, while those involving $\langle j_4\rangle_\kappa$, which depend on the direction of $\boldsymbol{\kappa}$, comprise the aspherical part.[67]

In terms of the occupation numbers

$$n(T_{2g}\sigma)=N^{-1}\sum_{n\mathbf{k}\text{ occ}}\sum_{\mu=1}^{3}|a_{n\mu\sigma}(\mathbf{k})|^2$$

and

$$n(E_g\sigma)=N^{-1}\sum_{n\mathbf{k}\text{ occ}}\sum_{\mu=4}^{5}|a_{n\mu\sigma}(\mathbf{k})|^2$$

of electrons of spin σ in T_{2g} and E_g orbitals, respectively, the d part of the form factor may be written as

$$f^{d\text{-}d}(\boldsymbol{\kappa})=f_{(s)}{}^{d\text{-}d}(\kappa)+f_{(a)}{}^{d\text{-}d}(\boldsymbol{\kappa})\,, \quad (6.11)$$

[66] R. J. Weiss and A. J. Freeman, J. Phys. Chem. Solids **10**, 147 (1959).

[67] It should be noted that Eq. (6.10) contains a small inconsistency. The quantities $\langle j_0\rangle$ and $\langle j_4\rangle$ depend on σ through the radial atomic functions $f^{\mu\sigma}(r)$ when they are obtained from an unrestricted Hartree-Fock atomic calculation. As a result, there should also be slight differences between the parameters E_0, Δ, A_1, $\cdots$, A_6 for $\uparrow$ and $\downarrow$ spins which presumably affect the $a_{n\mu\sigma}(\mathbf{k})$ but little, and have accordingly been neglected.

where it is convenient to write the spherical contribution in the form

$$f_{(s)}^{d\text{-}d}(\kappa)=\nu^{-1}[n(T_{2g}\uparrow)-n(T_{2g}\downarrow)]\langle j_0\rangle_\kappa^{T_{2g}\uparrow}+\nu^{-1}[n(E_g\uparrow)-n(E_g\downarrow)]\langle j_0\rangle_\kappa^{E_g\uparrow}+\nu^{-1}[n(T_{2g}\downarrow)][\langle j_0\rangle_\kappa^{T_{2g}\uparrow}-\langle j_0\rangle_\kappa^{T_{2g}\downarrow}]+\nu^{-1}[n(E_g\downarrow)][\langle j_0\rangle_\kappa^{E_g\uparrow}-\langle j_0\rangle_\kappa^{E_g\downarrow}], \quad (6.12)$$

and the aspherical contribution in the form

$$f_{(a)}^{d\text{-}d}(\kappa)=-\nu^{-1}A(hkl)[n(T_{2g}\uparrow)-n(T_{2g}\downarrow)]\langle j_4\rangle_\kappa^{T_{2g}\uparrow}+\tfrac{3}{2}\nu^{-1}A(hkl)[n(E_g\uparrow)-n(E_g\downarrow)]\langle j_4\rangle_\kappa^{E_g\uparrow}-\nu^{-1}A(hkl)n(T_{2g}\downarrow)[\langle j_4\rangle_\kappa^{T_{2g}\uparrow}-\langle j_4\rangle_\kappa^{T_{2g}\downarrow}]+\tfrac{3}{2}\nu^{-1}A(hkl)n(E_g\downarrow)[\langle j_4\rangle_\kappa^{E_g\uparrow}-\langle j_4\rangle_\kappa^{E_g\downarrow}]. \quad (6.13)$$

In Eqs. (6.12) and (6.13) the majority and minority spins have been represented by ↑ and ↓, respectively. The contributions of unpaired majority-spin electrons are given by the first two terms in each of the Eqs. (6.12) and (6.13), and the remaining terms represent the contributions of paired electrons. As stated previously, it is reasonable to expect the contribution of unpaired d electrons to be dominant; however, the contribution of the paired electrons is not negligible, as we shall show.

The magnetic form factor has been calculated from Eq. (6.1) and compared in Fig. 13 with the experimental results of Mook and Shull.[23] The normalized core polarization form factor $f_{\text{core}}(\kappa)$ is that of Watson and Freeman.[42] The orbital contribution $((g-2)/g)f_{\text{orb}}(\kappa)$ has been computed using results given by Blume.[64] The calculation of $f^{d\text{-}d}(\kappa)$ from Eqs. (6.11)–(6.13) has been carried out using the occupation numbers given in Table III and values of $\langle j_0\rangle_\kappa^{\mu\sigma}$ and $\langle j_4\rangle_\kappa^{\mu\sigma}$ computed from unrestricted Hartree-Fock atomic functions for a spin-polarized Ni^{++} ion in a cubic field.[68] The Ni^{++} results constitute a better choice than corresponding ones for Ni^{+}, whose $3d^9$ configuration more nearly approximates that present in the crystal, since the Ni^{++} wave functions better approximate the contracted wave functions near the top of the d band.

The contribution of the paired electrons, as computed from the last two terms in Eq. (6.12), is indicated by the solid curve in Fig. 13. Although in principle there is an aspherical contribution from these electrons, as indicated by the last two terms in Eq. (6.13), its magnitude is actually never larger than 0.001 and may be neglected. The unrestricted Hartree-Fock atomic functions of Watson and Freeman,[42] which form the basis functions for the present calculations, are contracted for majority (↑) spins relative to minority (↓) spins. Thus the majority-spin form factor is expanded relative to that of the minority spins and the difference $\langle j_0\rangle_\kappa^{\mu\uparrow}-\langle j_0\rangle_\kappa^{\mu\downarrow}$ is positive, except at large reflections, where it is small in any case. In our calculations, therefore, the paired electrons make a positive contribution to the spherical part of the form factor, as may be seen from Eq. (6.12).

[68] A. J. Freeman (private communication).

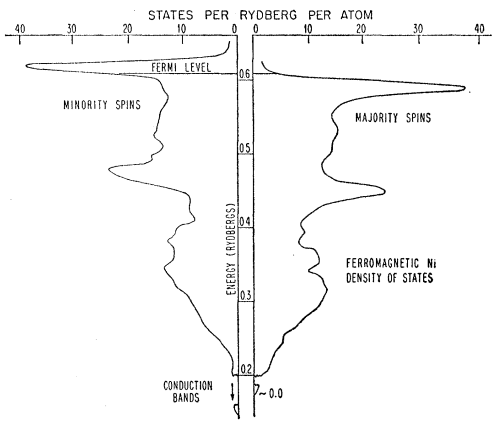

FIG. 12. Densities of states for minority- and majority-spin electrons in ferromagnetic Ni. The lower parts of the conduction bands are only shown schematically because the exact relative positions of the Γ_1 levels corresponding to majority and minority spins are uncertain.

The agreement of the calculated form factor with experiment as shown in Fig. 13 is good except at the three lowest reflections. At large reflections, the main contribution arises from $f_{(a)}^{d\text{-}d}$. The fraction of unpaired majority-spin electrons in E_g orbitals must be close to 14% if such good agreement is to be obtained, so long as the net conduction-electron polarization is not too large. This point was discussed in Sec. V, where it was shown that this fraction depends sensitively on the band structure and should be regarded as input information. Accordingly, the present calculation of the magnetic form factor is somewhat circular in that the parameter Δ has been adjusted in Sec. VB to secure agreement with its aspherical part. However, this very fact again emphasizes in very specific terms how neutron-diffraction results may be used directly in connection with band (in contrast to pseudo-atomic) representations of the electronic energy levels of solids

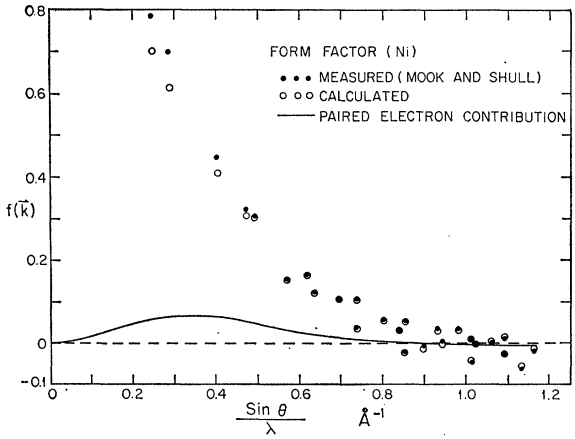

FIG. 13. Comparison of calculated magnetic form factor of Ni with experimental results of Mook and Shull (Ref. 23). Solid line indicates contribution of paired electrons obtained from unrestricted Hartree-Fock atomic wave functions of Watson and Freeman (Ref. 42).

to obtain extremely fine adjustments of the d-band complex.

There are several reasons why discrepancies may be expected to occur between the calculated and measured values of the form factor. One reason is that unrestricted conduction-band wave functions have not been used in the present work. It was pointed out in Sec. V.A that the spin density of the conduction electrons may be expected to vary spatially, and even change sign, presumably giving rise to the negative spin density in the outer parts of the unit cell indicated in Fig. 9. Another reason is that it is difficult to obtain a good estimate of the contribution arising from paired electrons. This contribution depends crucially on the exact form of the unrestricted d-band wave functions over the whole range of d-band energies. Since LCAO's are good only near the top of the d-band complex, it is not really correct to use them throughout the d bands, as we have done in calculating the form factor shown in Fig. 13. It will be noted from Fig. 13 that the contribution of paired electrons is most important at the lower reflections, where the discrepancies between the calculated and measured form factors are largest. In addition, it should be remembered that there are several terms in the form factor that have been neglected but which may contribute appreciably. In particular, the OPW-d terms, as mentioned above, appear to be largest in the vicinity of the first few reflections, although their magnitude has not been estimated.

[*Note added in Proof.* Further light has recently been shed on the Fermi surface of ferromagnetic Ni by the independent de Haas–van Alphen studies of Tsui and Stark[69] and of Stone and Gold.[70] Their data has confirmed the existence of the necks at L first observed by Joseph and Thorsen.[9] The new oscillations found by these experimenters[69,70] have been interpreted in terms of hole pockets at X arising from the position of the X_5 level. These pockets are shaped like fluted ellipsoids, as would be expected from the present band structure. However, their dimensions are roughly 15% greater than those which may be read off Fig. 11, implying that the X_5 level in Fig. 10 is approximately 0.003 Ry too low. No (conclusive) evidence has been found in the de Haas-van Alphen data for hole pockets at X arising from the X_2 level. The absence of these pockets would imply that X_2 is below the Fermi level, or roughly 0.005 Ry below its position in the present calculations; this would require some minor adjustments in the parameters of the interpolation scheme. There does not appear to be any conclusive evidence regarding the presence or absence of minority hole pockets at L, (although Tsui and Stark[69] have reported data points which might correspond to them). We are grateful to A. V. Gold and D. R. Stone for discussing their results with us prior to publication, and to Dr. G. Weisz for helpful comments.]

ACKNOWLEDGMENTS

We are grateful for a number of stimulating discussions with R. V. Jones, A. J. Freeman, and H. A. Mook. Helpful comments from H. Brooks, J. Friedel, C. Herring, J. H. Van Vleck, and S. Potter are also deeply appreciated.

[69] D. C. Tsui and R. W. Stark, Phys. Rev. Letters **17**, 871 (1966).

[70] D. R. Stone and A. V. Gold (private communication), and (to be published).